regulation of important cellular transcription factors such as nuclear factor-κB (NF-κB) (Rossi et al., 1997) and proliferator-activated receptor γ (PPAR γ) (Hayes et al., 2002).

In this study, we report that PGA_1 inhibits the Vif-mediated degradation of A3G in human cells. Induction of HSP70 is associated with inhibition of Vif-dependent polyubiquitination of A3G, which results in selective inhibition of Vif-mediated A3G degradation.

We used a tetrazolium-based MTS assay to determine the viability of 293T cells in the presence of PGA_1 (Supplementary Mate-

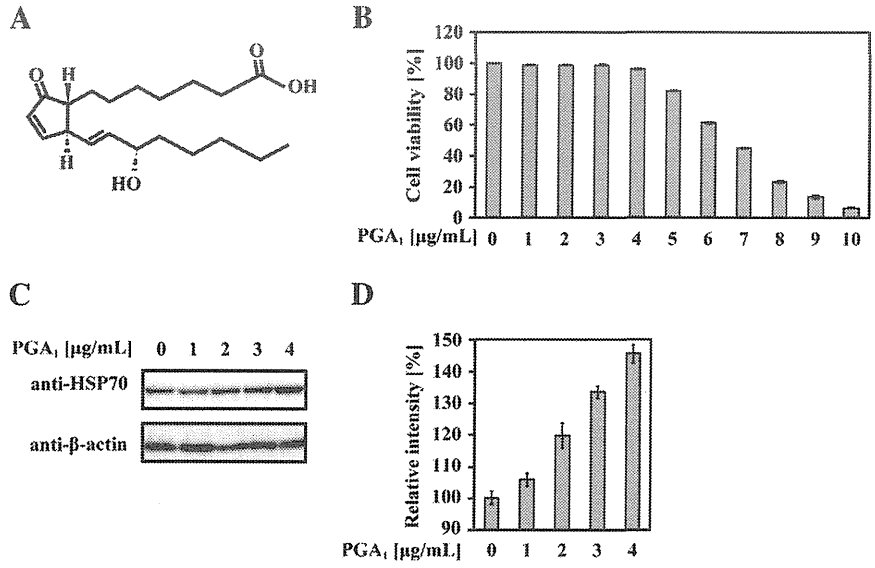

Fig. 1. Induction of HSP70 synthesis by PGA_1. (A) Structure of cyclopentenone prostaglandin A_1 (PGA_1). (B) The cytotoxic effect of PGA_1 (Biomol GmbH) in 293T cells, shown as the percentage reduction of viable cell numbers as assessed in a tetrazolium-based MTS assay. The results are representative of three independent experiments, and error bars show the standard deviations of the means. (C) 293T cells (5×10^5) were treated with 1–4 μg/mL PGA_1. After 24 h, the cell lysates were harvested, and samples containing the same amounts of protein were separated by SDS–PAGE and processed for immunoblot analysis using an anti-HSP70 monoclonal antibody. (D) The relative intensity of HSP70 bands was determined by densitometry. Results are representative of three independent experiments, and error bars show the standard deviations of the means.

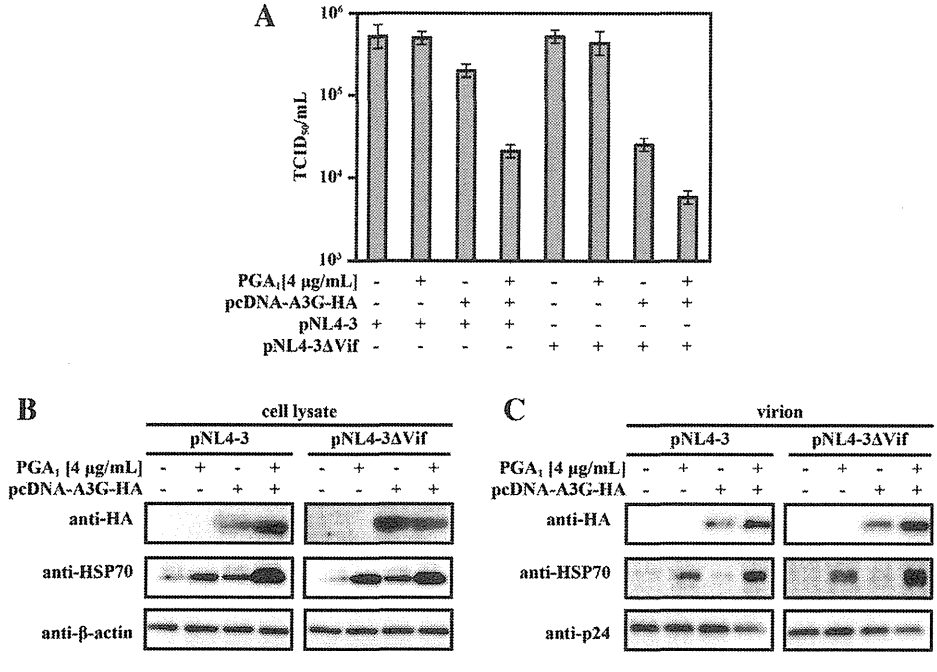

Fig. 2. Induction of HSP70 synthesis by PGA_1 regulates HIV-1 infectivity in an A3G-dependent manner. (A) 293T cells (5×10^5) were treated with 4 μg/mL PGA_1 (+) or control diluents (−) for 4 h. The cells were co-transfected with 0.1 μg of pNL4-3 or pNL4-3-delta-Vif and 1.0 μg of pcDNA-A3G-HA or pcDNA3.1 (empty plasmid) using Lipofectamine 2000 (Invitrogen). At 48 h post-transfection, the supernatants were harvested, and the amount of each virus was normalized to the equivalent level of p24 Gag antigen. MAGI cells (1×10^4) were infected with each virus (corresponding to 5 ng of p24 Gag antigen), and infected cells were stained with X-Gal 2 days later. The 50% tissue culture infective dose ($TCID_{50}$) was determined for the last dilution of each virus that was capable of infecting the cells. The results are representative of three independent experiments, and error bars show the standard deviations of the means. (B and C) Each stock of cell lysate or virus in Figure 2A was subjected to western blotting and then analyzed with the indicated antibody.

rials and Methods). Dose-dependent cytotoxicity was not observed upon application of PGA_1 (99% at concentrations ranging between 1 and 4 μg/mL) (Fig. 1B). Next, we investigated whether PGA_1 affects HSP70 synthesis. 293T cells were treated with PGA_1 (1–4 μg/mL), and the level of HSP70 protein was examined by western blot. PGA_1 treatment significantly increased HSP70 expression in 293T cells (Fig. 1C and D). Furthermore, we examined whether the induction of HSP70 synthesis by PGA_1 influenced A3G function. Either pNL4-3 or pNL4-3-delta-Vif was transfected into 293T cells along with either pcDNA3.1 (empty plasmid) or pcDNA-A3G-HA in the absence or presence of PGA_1. Viral infectivity was measured using the MAGI assay (Supplementary Materials and Methods). As shown in Figure 2A, the PGA_1-treated 293T cells clearly suppressed the infectivity of wild-type HIV-1 in the presence of A3G. In the absence of A3G, PGA_1 did not affect the infectivity of wild-type HIV-1. As expected, the induction of HSP70 by PGA_1 in A3G-HA-transfected 293T cells led to an inhibition of the infectivity of Vif-deficient HIV-1 (Fig. 2A). Moreover, HSP70 induction had no effect on the infectivity of the Vif-deficient HIV-1 particles produced by mock-transfected 293T cells.

To demonstrate whether HSP70 induction by PGA_1 affects the packaging of A3G into virions, cell lysates and viruses were analyzed for A3G expression by western blotting. The 293T cells treated with PGA_1 showed a significant increase in the amount of intracellular and wild-type virion-associated A3G (Fig. 2B and C). Interestingly, HSP70 induction by PGA_1 enhanced the level of A3G packaging in Vif-deficient virions but had no effect on intracellular A3G and viral release (Fig. 2B and C). These results indicate that HSP70 induction by PGA_1 blocked Vif-mediated A3G degradation and enhanced the incorporation of A3G into both wild-type and Vif-deficient virions. (Sugiyama et al., 2011).

Importantly, HSP70 had no effect on the expression of A3G in 293T cells transfected with the Vif-deleted HIV-1 proviral plasmid (Fig. 2B). Our results suggest that HSP70 induction by PGA_1 may inhibit the degradation of A3G by Vif. To further investigate whether our findings have physiological relevance in cells expressing endogenous A3G, we used H9 cells. First, we investigated whether PGA_1 affects HSP70 synthesis in H9 cells. The cells were treated with PGA_1 (4 μg/mL), and the level of HSP70 protein was examined by western blot. PGA_1 treatment significantly increased the amount of HSP70 in uninfected H9 cells (Fig. 3A), but there was no difference in A3G expression after PGA_1 treatment (Fig. 3A). H9 cells were challenged with NL4-3 or NL4-3-delta-Vif viruses, which corresponded to 5 ng of p24 Gag antigen. After incubation at 37 °C for 4 h, the cells were washed three times in PBS and treated with PGA_1 (4 μg/mL). For some cultures, PGA_1 treatment was repeated at 48 h post-infection. After 96 h, the cell lysates were harvested and analyzed by western blotting. When H9 cells were infected with NL4-3, the level of endogenous A3G and HSP70 were enhanced by a single PGA_1 treatment (Fig. 3B, compare lanes 1 and 2). Repeated PGA_1 treatments had no effect on the level of endogenous A3G and HSP70 compared with a single PGA_1 treatment (Fig. 3B, lane 2 [a single PGA_1 treatment] and lane 3 [repeated PGA_1 treatments]). In contrast, in NL4-3-delta-Vif-infected H9 cells, PGA_1 did not have a significant effect on the level of endogenous A3G (Fig. 3D, compare lanes 1 and 2 [a single PGA_1 treatment]

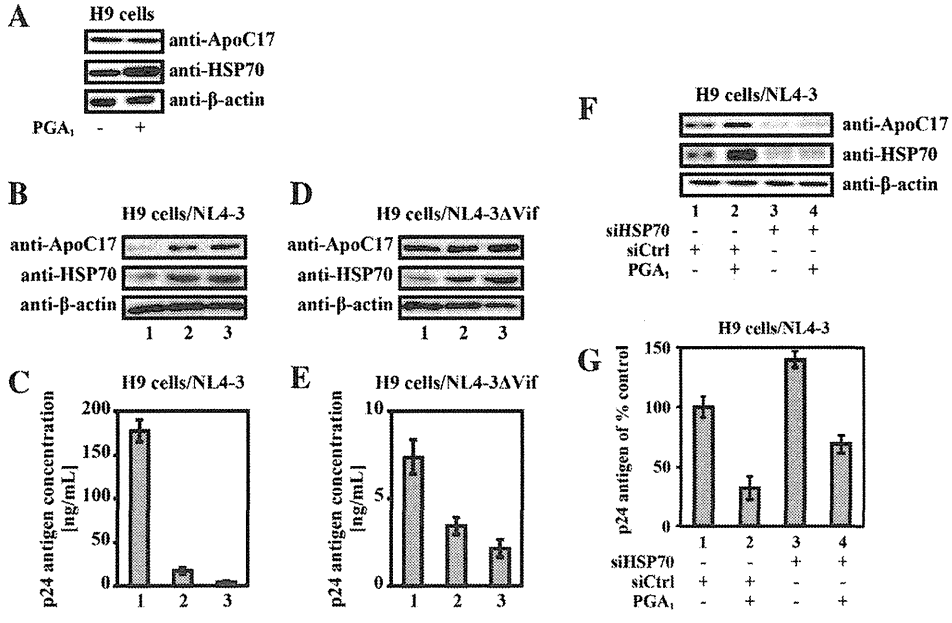

Fig. 3. PGA_1 affects the level of endogenous A3G expression in non-permissive T cells expressing HIV-1 Vif. (A) HSP70 synthesis and A3G expression by PGA_1. H9 cells (5×10^5) were treated with 4 μg/mL PGA_1. After 48 h, the cell lysates were harvested, and samples containing the same amounts of protein were separated by SDS–PAGE and processed for immunoblot analysis using anti-HSP70 and anti-ApoC17 monoclonal antibodies. (B-E) H9 cells (1×10^6) were challenged with wild-type (NL4-3) or Vif-defective (NL4-3-delta-Vif) virus particles (corresponding to 5 ng of p24 Gag antigen). After incubation at 37 °C for 4 h, the cells were washed three times in PBS and then treated with 4 μg/mL PGA_1. For some cultures, PGA_1 treatment was repeated at 48 h post-infection. After 96 h, the cell lysates were harvested and analyzed by western blotting with the indicated antibodies (B, D). Lane 1: no PGA_1 treatment; lane 2: a single PGA_1 treatment; lane 3: repeated PGA_1 treatments. (C, E) p24 Gag antigen levels in supernatants were determined after 96 h using an ELISA-based system. The amount of p24 Gag antigen was quantified with LUMIPULSE®*f* (forte), a fully automated chemiluminescent enzyme immunoassay (CLEIA) system (Fujirebio) (Sakai et al., 1999). Lane 1: no PGA_1 treatment; lane 2: a single PGA_1 treatment; lane 3: repeated PGA_1 treatments. The results are representative of three independent experiments, and error bars show the standard deviations of the means. (F, G) H9 cells (1×10^6) were transfected with 100 nM control siRNA (siCtrl) or 100 nM HSP70-specific siRNA (siHSP70) using Lipofectamine 2000 for 4 h. The cells were then challenged with NL4-3 (corresponding to 5 ng of p24 Gag antigen). After incubation at 37 °C for 4 h, the cells were washed three times in PBS and treated with PGA_1 (4 μg/mL). After 48 h, the cell lysates were harvested and analyzed by western blotting with the indicated antibodies (F). Lane 1, 3: no PGA_1 treatment; lane 2, 4: PGA_1 treatment. (G) p24 Gag antigen levels in supernatants were determined after 48 h using the CLEIA system (LUMIPULSE®*f*). Lane 1, 3: no PGA_1 treatment; lane 2, 4: PGA_1 treatment. The vertical axis of the inset represents the percentage concentration of p24 Gag antigen compared with the control (lane 1). The results are representative of three independent experiments, and error bars show the standard deviations of the means.

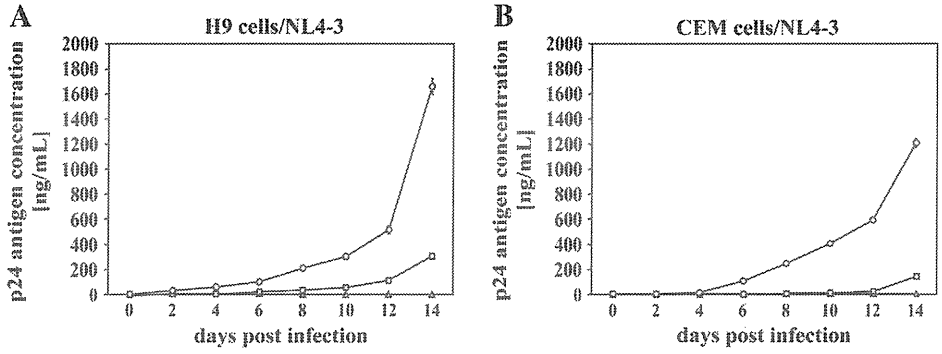

Fig. 4. PGA_1 suppresses long-term HIV-1 replication in non-permissive T cells. (A) H9 cells (1×10^6) or (B) CEM cells (1×10^6) were challenged with NL-4-3 (corresponding to 5 ng of p24 Gag antigen). After incubation at 37 °C for 4 h, the cells were washed three times in PBS and then treated with 4 μg/mL PGA_1 on day 0 or every 2 days for 14 days. To monitor HIV-1 production, the p24 Gag antigen concentration in supernatants was measured using the CLEIA system (LUMIPULSE®*f*). Single PGA_1 treatment (white squares), repeated PGA_1 treatments (white triangles), and control (white circle). The results are representative of three independent experiments, and error bars show the standard deviations of the means.

with lane 3 [repeated PGA_1 treatments]) but did affect the virion packaging of A3G (see Fig. 2C). The PGA_1-mediated anti-HIV-1 effect was examined by measuring p24 Gag antigen levels after 96 h. p24 Gag antigen levels were dramatically reduced in cells treated once or repeatedly with PGA_1 compared with the control when cells were infected with NL4-3 (Fig. 3C). In addition, inhibitory effect of PGA_1 reduced in H9 cells infected with Vif-deficient HIV-1 (Fig. 3E). There was no significant decrease in cell viability between treatment groups, as assessed by a tetrazolium-based MTS assay (data not shown).

To further investigate the influence of HSP70 silencing on PGA_1-mediated anti-HIV-1 effects, H9 cells were transfected with control siRNA (siCtrl) or HSP70-specific siRNA (siHSP70) (Supplementary Materials and Methods) and were then challenged with NL4-3 (corresponding to 5 ng of p24 Gag antigen). After incubation at 37 °C for 4 h, the cells were washed three times in PBS and treated with PGA_1 (4 μg/mL). As shown Fig. 3F, the knockdown of HSP70 expression in PGA_1-untreated H9 cells significantly decreased the amount of A3G (compare lanes 1 and 3), whereas the p24 Gag antigen levels were slightly increased (Fig. 3G, compare lanes 1 and 3). We think the enhancement of p24 Gag antigen expression is due to Vif-mediated degradation of endogenous A3G by the knockdown of HSP70. However, the knockdown of HSP70 in PGA_1-treated H9 cells (Fig. 3G, lane 4) decreased the amount of p24 Gag antigen compared with HSP70 knockdown in PGA_1-untreated H9 cells (Fig. 3G, lane 3). This effect may occur by the regulation of two important cellular transcription factors: nuclear factor-κB (NF-κB) (Rossi et al., 1997) and proliferator-activated receptor γ (PPAR γ) (Hayes et al., 2002). However, anti-HIV-1 effects of PGA_1 were constantly more prominent in H9 cells transfected with siCtrl (about 70% inhibition) than with siHSP70 (about 50% inhibition). These results suggest that the induction of HSP70 by PGA_1 suppressed Vif-mediated degradation of endogenous A3G in non-permissive cells.

Finally, we examined the effect of PGA_1 on HIV-1 replication over time. When H9 or CEM cells were infected with NL4-3 and then treated with PGA_1 (4 μg/mL), the levels of p24 Gag antigen were reduced through day 6 (H9 cells) or 8 (CEM cells) but had increased slightly by day 8 (H9 cells) or 10 (CEM cells) (Fig. 4A and B, white squares). However, when PGA_1 (4 μg/mL) was added to the cells at 2-day intervals for 14 days (white triangles), the significant reduction in p24 Gag antigen was sustained through day 14.

In conclusion, we found that the induction of HSP70 synthesis by PGA_1 blocks Vif-mediated A3G degradation and enhances the incorporation of A3G into both wild-type and Vif-deficient virions. PGA_1 inhibits HIV-1 replication, at least in part, by blocking Vif-mediated A3G degradation. These results suggest that a new mechanism used by prostaglandins may aid in the search for novel anti-retroviral drugs.

Acknowledgments

We thank Dr. Darlene Chen for providing pcDNA-A3G-HA and Haruki Naganuma and Hiroshi Koseki for their technical assistance. This work was supported in part by the following: a Grant-in-Aid for Science Research (C) from the Japan Society for the Promotion of Science (JSPS), Japan; a Grant-in-Aid for AIDS research from the Ministry of Health, Labor, and Welfare, Japan; and a Grant from the Strategic Research Foundation Grant-aided Project for Private Universities from the Ministry of Education, Culture, Sport, Science, and Technology, Japan (MEXT).

Appendix A. Supplementary material

Supplementary data associated with this article can be found, in the online version, at http://dx.doi.org/10.1016/j.antiviral.2013.06.017.

References

Amici, C., Santoro, M.G., 1991. Suppression of virus replication by prostaglandin A is associated with heat shock protein synthesis. J. Gen. Virol. 72 (Pt 8), 1877–1885.
Ankel, H., Mittnacht, S., Jacobsen, H., 1985. Antiviral activity of prostaglandin A on encephalomyocarditis virus-infected cells: a unique effect unrelated to interferon. J. Gen. Virol. 66 (Pt 11), 2355–2364.
Barouch, D.H., 2008. Challenges in the development of an HIV-1 vaccine. Nature 455, 613–619.
Carattoli, A., Fortini, D., Rozera, C., Giorgi, C., 2000. Inhibition of HIV-1 transcription by cyclopentenone prostaglandin A1 in Jurkat T lymphocytes. J. Biol. Regul. Homeost. Agents 14, 209–216.
D'Onofrio, C., Alvino, E., Garaci, E., Bonmassar, E., Santoro, M.G., 1990. Selection of HTLV-I positive clones is prevented by prostaglandin A in infected cord blood cultures. Br. J. Cancer 61, 207–214.
Harris, R.S., Bishop, K.N., Sheehy, A.M., Craig, H.M., Petersen-Mahrt, S.K., Watt, I.N., Neuberger, M.S., Malim, M.H., 2003. DNA deamination mediates innate immunity to retroviral infection. Cell 113, 803–809.
Hayes, M.M., Lane, B.R., King, S.R., Markovitz, D.M., Coffey, M.J., 2002. Peroxisome proliferator-activated receptor gamma agonists inhibit HIV-1 replication in macrophages by transcriptional and post-transcriptional effects. J. Biol. Chem. 277, 16913–16919.
Hirayama, E., Hattori, M., Kim, J., 2006. Specific binding of heat shock protein 70 with HN-protein inhibits the HN-protein assembly in Sendai virus-infected Vero cells. Virus Res. 120, 199–207.
Iwatani, Y., Chan, D.S., Wang, F., Maynard, K.S., Sugiura, W., Gronenborn, A.M., Rouzina, I., Williams, M.C., Musier-Forsyth, K., Levin, J.G., 2007. Deaminase-independent inhibition of HIV-1 reverse transcription by APOBEC3G. Nucleic Acids Res. 35, 7096–7108.

Kobayashi, M., Takaori-Kondo, A., Miyauchi, Y., Iwai, K., Uchiyama, T., 2005. Ubiquitination of APOBEC3G by an HIV-1 Vif-Cullin5-Elongin B-Elongin C complex is essential for Vif function. J. Biol. Chem. 280, 18573–18578.

Mehle, A., Goncalves, J., Santa-Marta, M., McPike, M., Gabuzda, D., 2004. Phosphorylation of a novel SOCS-box regulates assembly of the HIV-1 Vif-Cul5 complex that promotes APOBEC3G degradation. Genes Dev. 18, 2861–2866.

Mercenne, G., Bernacchi, S., Richer, D., Bec, G., Henriet, S., Paillart, J.C., Marquet, R., 2010. HIV-1 Vif binds to APOBEC3G mRNA and inhibits its translation. Nucleic Acids Res. 38, 633–646.

Nathans, R., Cao, H., Sharova, N., Ali, A., Sharkey, M., Stranska, R., Stevenson, M., Rana, T.M., 2008. Small-molecule inhibition of HIV-1 Vif. Nat. Biotechnol. 26, 1187–1192.

Robb, M.L., 2008. Failure of the Merck HIV vaccine: an uncertain step forward. Lancet 372, 1857–1858.

Rossi, A., Elia, G., Santoro, M.G., 1997. Inhibition of nuclear factor kappa B by prostaglandin A1: an effect associated with heat shock transcription factor activation. Proc. Natl. Acad. Sci. USA 94, 746–750.

Sakai, A., Hirabayashi, Y., Aizawa, S., Tanaka, M., Ida, S., Oka, S., 1999. Investigation of a new p24 antigen detection system by the chemiluminescence-enzyme-immuno-assay. Kansenshogaku Zasshi 73, 205–212.

Santoro, M.G., 1997. Antiviral activity of cyclopentenone prostanoids. Trends Microbiol. 5, 276–281.

Santoro, M.G., Benedetto, A., Carruba, G., Garaci, E., Jaffe, B.M., 1980. Prostaglandin A compounds as antiviral agents. Science 209, 1032–1034.

Santoro, M.G., Jaffe, B.M., Garaci, E., Esteban, M., 1982. Antiviral effect of prostaglandins of the A series: inhibition of vaccinia virus replication in cultured cells. J. Gen. Virol. 63, 435–440.

Santoro, M.G., Jaffe, B.M., Esteban, M., 1983. Prostaglandin A inhibits the replication of vesicular stomatitis virus: effect on virus glycoprotein. J. Gen. Virol. 64 (Pt 12), 2797–2801.

Santoro, M.G., Favalli, C., Mastino, A., Jaffe, B.M., Esteban, M., Garaci, E., 1988. Antiviral activity of a synthetic analog of prostaglandin A in mice infected with influenza A virus. Arch. Virol. 99, 89–100.

Santoro, M.G., Garaci, E., Amici, C., 1989. Prostaglandins with antiproliferative activity induce the synthesis of a heat shock protein in human cells. Proc. Natl. Acad. Sci. USA 86, 8407–8411.

Sheehy, A.M., Gaddis, N.C., Choi, J.D., Malim, M.H., 2002. Isolation of a human gene that inhibits HIV-1 infection and is suppressed by the viral Vif protein. Nature 418, 646–650.

Sheehy, A.M., Gaddis, N.C., Malim, M.H., 2003. The antiretroviral enzyme APOBEC3G is degraded by the proteasome in response to HIV-1 Vif. Nat. Med. 9, 1404–1407.

Stopak, K., de Noronha, C., Yonemoto, W., Greene, W.C., 2003. HIV-1 Vif blocks the antiviral activity of APOBEC3G by impairing both its translation and intracellular stability. Mol. Cell 12, 591–601.

Sugiyama, R., Nishitsuji, H., Furukawa, A., Katahira, M., Habu, Y., Takeuchi, H., Ryo, A., Takaku, H., 2011. Heat shock protein 70 inhibits HIV-1 Vif-mediated ubiquitination and degradation of APOBEC3G. J. Biol. Chem. 286, 10051–10057.

Yamamoto, N., Fukushima, M., Tsurumi, T., Maeno, K., Nishiyama, Y., 1987. Mechanism of inhibition of herpes simplex virus replication by delta 7-prostaglandin A1 and delta 12-prostaglandin J2. Biochem. Biophys. Res. Commun. 146, 1425–1431.

Yu, X., Yu, Y., Liu, B., Luo, K., Kong, W., Mao, P., Yu, X.F., 2003. Induction of APOBEC3G ubiquitination and degradation by an HIV-1 Vif-Cul5-SCF complex. Science 302, 1056–1060.

Yu, Y., Xiao, Z., Ehrlich, E.S., Yu, X., Yu, X.F., 2004. Selective assembly of HIV-1 Vif-Cul5-ElonginB-ElonginC E3 ubiquitin ligase complex through a novel SOCS box and upstream cysteines. Genes Dev. 18, 2867–2872.

Zhang, H., Yang, B., Pomerantz, R.J., Zhang, C., Arunachalam, S.C., Gao, L., 2003. The cytidine deaminase CEM15 induces hypermutation in newly synthesized HIV-1 DNA. Nature 424, 94–98.

Zuo, T., Liu, D., Lv, W., Wang, X., Wang, J., Lv, M., Huang, W., Wu, J., Zhang, H., Jin, H., Zhang, L., Kong, W., Yu, X., 2012. Small-molecule inhibition of human immunodeficiency virus type 1 replication by targeting the interaction between Vif and ElonginC. J. Virol. 86, 5497–5507.

JVI
Journals.ASM.org

A Carboxy-Terminally Truncated Human CPSF6 Lacking Residues Encoded by Exon 6 Inhibits HIV-1 cDNA Synthesis and Promotes Capsid Disassembly

Takanori Hori, Hiroaki Takeuchi, Hideki Saito, Ryuta Sakuma, Yoshio Inagaki, Shoji Yamaoka

Department of Molecular Virology, Tokyo Medical and Dental University, Tokyo, Japan

Since HIV-1 replication is modulated at multiple stages by host cell factors, identification and characterization of those host cell factors are expected to contribute to the development of novel anti-HIV therapeutics. Previous studies showed that a C-terminally truncated cytosolic form of cleavage and polyadenylation-specific factor 6 (CPSF6-358) inhibits HIV-1 infection through interference with HIV-1 trafficking to the nucleus. Here we identified and characterized a different configuration of C-terminally truncated human CPSF6 (hCPSF6-375) through cDNA expression cloning coupled with ganciclovir-mediated lethal selection. Notably, hCPSF6-375, but not mouse CPSF6-358 (mCPSF6-358) as previously reported, remarkably interfered with viral cDNA synthesis after HIV-1 infection. Moreover, we found that hCPSF6-375 aberrantly accelerated the disassembly of the viral capsid in target cells, while CPSF6-358 did not. Sequence comparison of CPSF6-375 and CPSF6-358 cDNAs showed a lack of exon 6 and additional coding sequence for 54 amino acid residues in the C terminus of hCPSF6-375. Mutational analyses revealed that the residues encoded by exon 6, but not the C-terminal 54 residues in hCPSF6-375, is responsible for impaired viral cDNA synthesis by hCPSF6-375. This is the first report demonstrating a novel mode of HIV-1 inhibition by truncated forms of CPSF6 that involves rapid capsid disassembly and inhibition of viral cDNA synthesis. These findings could facilitate an increased understanding of viral cDNA synthesis in light of the viral capsid disassembly.

Human immunodeficiency virus type 1 (HIV-1) replication requires the help of host cell factors, and diverse cellular pathways are hijacked by HIV-1 for efficient completion of the viral replication cycle (1). A wide range of cellular factors and processes are exploited by HIV-1 during various stages of replication, which involves the uncoating steps that form into a reverse transcription complex, intracellular trafficking of the viral preintegration complex (PIC) to the cell nucleus, and integration of the viral DNA into a host cell chromosome for generation of the provirus (2). Several genome-wide small interfering RNA (siRNA) analyses have demonstrated over 250 cellular factors that influence HIV-1 infection (3–5). On the other hand, cDNA expression cloning also proved to be a powerful strategy for discovering functional properties of cellular genes that may potentially contribute to identification of host targets for anti-HIV therapeutics (6–10). By screening with a mouse cDNA expression library, a C-terminally truncated form of mouse cleavage and polyadenylation-specific factor 6 (mCPSF6) was recently identified as a novel functional protein that blocks HIV-1 trafficking to the nucleus (7). The truncated protein, mCPSF6-358, reduced the amount of the 2-long terminal repeat (LTR) circular form of viral DNA that is located in the nucleus, but not the late product of viral cDNA, indicating impairment of the nuclear entry of HIV-1 (7). More recently, it was shown that the C-terminal 58 residues of mCPSF6-358 are sufficient for HIV-1 inhibition and that mCPSF6-358 residues 313 to 327 contribute to antiviral activity (11). A subsequent report showed that a synthesized peptide corresponding to mCPSF6 (residues 313 to 327) binds specifically to the N-terminal domain of HIV-1 capsid (12). However, it has remained unclear how the capsid–mCPSF6-358 interaction interferes with the nuclear import of the viral PIC.

Recent studies suggest that proper uncoating is a key step for reverse transcription. (i) In the case of restriction of HIV-1 by rhesus monkey TRIM5α, productive reverse transcription is abrogated by accelerated disassembly of viral capsids (13). (ii) The Vif, Nef, and integrase proteins are essential for optimal stability of the viral core that leads to efficient viral cDNA synthesis in target cells (14–16). (iii) Capsid mutations that impair HIV-1 infection are unable to achieve proper uncoating and reverse transcription (17–20). Overall, these observations suggest that proper uncoating is functionally linked to reverse transcription of HIV-1.

In the present study, we identified a novel C-terminally truncated form of human CPSF6 (hCPSF6) lacking residues encoded by exon 6 (Ex6), hCPSF6-375, by lethal selection of cells resistant to HIV infection following transduction of a human cDNA expression library and focused on its ability to inhibit viral cDNA synthesis in light of the viral capsid disassembly.

MATERIALS AND METHODS

Cells. HEK293, HeLa, and Plat-E packaging cells (21) were propagated in Dulbecco's modified Eagle's medium containing 10% fetal bovine serum (FBS) and penicillin-streptomycin. MT-4/CCR5 and MOLT-4 cells were maintained in complete RPMI 1640 medium supplemented with 10% FBS and penicillin-streptomycin.

Preparation of virus stocks. HEK293T cells cultured in a 10-cm dish were cotransfected with 8 μg of pNL4-3luc (*env nef* mutant) (22) and 2 μg of pHCMV-G (vesicular stomatitis virus G protein [VSV-G]) using Fu-

Received 14 January 2013 Accepted 26 April 2013
Published ahead of print 8 May 2013
Address correspondence to Hiroaki Takeuchi, htake.molv@tmd.ac.jp, or Shoji Yamaoka, shojimmb@tmd.ac.jp.
T.H. and H.T. contributed equally to this article.

doi:10.1128/JVI.00124-13

GENE 6 (Roche Applied Science, Mannheim Germany) according to the manufacturer's instructions. Virus supernatant was harvested at 48 h posttransfection and filtered through a 0.45-μm-pore syringe filter. HIV-1_{NL4-3} virus stock was prepared by transfection of HeLa cells as previously reported (23). Titers of the virus stocks were quantitated by HIV-1 CA (p24) enzyme-linked immunosorbent assay (ELISA) (ZeptMetrix Corporation, Buffalo, NY) and by determination of the reverse transcriptase (RT) activity (24). For production of retrovirus vectors, Plat-E cells were cotransfected with retrovirus vector plasmids and VSV-G using FuGENE 6 transfection reagent. Culture supernatant of Plat-E cells was collected 60 h after transfection and filtered through a 0.45-μm-pore syringe filter.

Construction of cDNA library and screening. Construction of the retroviral cDNA library was performed as described previously (25). Briefly, complementary DNAs were synthesized from poly(A) RNA of MT-1 cells with random hexamer primers using the SuperScript Choice system (Invitrogen) according to the manufacturer's instructions. The synthesized cDNAs were inserted between the BstXI sites of pMRX (26) using BstXI adaptors (Invitrogen), generating a retroviral cDNA expression library. HEK293 cells were transduced with VSV-G-pseudotyped retroviruses expressing this cDNA library. The cells were then infected with VSV-G-pseudotyped NL4-3 thymidine kinase (NL4-3-TK) vector (*env nef* mutant) and subjected to lethal selection with ganciclovir (GCV) (2 μg/ml) to exclude cells infected with the NL4-3-TK vector. After the repeated infection and selection, susceptibility to HIV-1 infection was assessed by infection with NL4-3luc vector and genomic DNA was isolated from surviving cell pools. Inserted cDNAs were amplified by PCR from the genomic DNA, cloned into pCR2.1 (Invitrogen), and sequenced. The cDNA was subcloned into the pMRX-HA-ires-puro vector (27), generating pMRX-HA-hCPSF6-375. Mutated nucleotides were corrected to match the reference sequence (NM_007007.2) by site-directed mutagenesis.

Construction of expression vectors. An *env*-defective variant of HIV-1 NL4-3, pNL4-3*env*(−) carrying a 580-bp deletion between the BglII restriction site in the *env* gene, was constructed. To generate a herpes simplex virus thymidine kinase (HSV-TK) gene-carrying NL4-3*env*(−) vector, the last 133 bp of the *env* gene was amplified from pNL4-3 using *Pfu* DNA polymerase (Stratagene, La Jolla, CA) with the following primers: 5′-TCTAGAATTCTCGAGTGTTAACTTGCTCAATGCCACAGCC ATAGC-3′ and 5′-GATGGCCGGGGTACGAAGCCATCTTATAGCAA AATCCTTTCCA-3′. The HSV-TK gene was amplified from the pIgκ2tkH vector (28) using *Pfu* DNA polymerase with the following primers: 5′-ATGGCTTCGTACCCCGGCCATCAACACGCGTC-3′ and 5′-CCGCTCGAGTTTCAGTTAGCC-3′. The fragments of the last 133 bp of the *env* gene and HSV-TK gene were fused by fusion PCR. After confirmation of the nucleotide sequence, fused DNA fragments were extracted after digestion with HpaI and XhoI and inserted into HpaI and XhoI sites of pNL4-3*env*(−), generating pNL4-3tk. pNL4-3 CA N74D-luc (*env* and *nef* negative) was generated by site-directed mutagenesis on pCR2.1 using the NL4-3 *gag* gene (nucleotides [nt] 689 to 2225) of the HIV-1_{NL4-3} genome (GenBank accession no. M19921) as the template. Primers NL4-3 CA-N74D-5 (5′-TTAAAAGAGACCATCGATGAGGAA GCTGCAGAA-3′) and NL4-3 CA-N74D-3 (5′-TTCTGCAGCTTCCTC ATCGATGGTCTCTTTTAA-3′) were used for N74D substitution. The mutated DNA fragment was inserted to the BssHII and ApaI sites of pNL4-3luc (*env nef* mutant). The resultant plasmid was referred to as pNL4-3 CA N74D-luc. For construction of murine CPSF6 mutant expression vectors, the cDNAs of murine CPSF6 variants were amplified by PCR using NIH 3T3 cell-derived cDNAs as the template. Primers BglII mCPSF6 F (5′-AAAGATCTGCCACCATGGCGGACGGTGTGGAC-3′) and mCPSF6 321R stop NotI (5′-AATGCGGCCGCCTAGCCTGGAGG TGGAGGTGGTC-3′) were used for amplification of mCPSF6-321 and mCPSF6-358. Primers BglII mCPSF6 F (5′-AAAGATCTGCCACCATGG CGGACGGTGTGGAC-3′) and m6CT 375 R stop NotI (5′-AATGCGGC CGCCTAACTATCTGATGTTGGCATGC-3′) were used for amplification of mCSPF6-375 and mCPSF6-412. The amplified cDNAs were inserted into pCR2.1 and sequenced. The cDNAs were inserted into the BamHI and NotI sites of pMRX-IRES-puro (29). The resultant plasmids were referred to as pMRX-mCPSF6-321, pMRX-mCPSF6-358, pMRX-mCPSF6-375, and pMRX-mCPSF6-412, respectively. For generation of human CPSF6 mutant expression constructs, the cDNAs of hCPSF6-321 and hCPSF6-375 were amplified by PCR using pMRX-HA-hCPSF6-375 as the template. Primers BamHI hCPSF6 F (5′-AAGGATCCGCCACCA TGGCGGACGGCGTGGACCAC-3′) and hCPSF6 321R stop NotI (5′-A ATGCGGCCGCCTAGCCTGGAGGTGGAGGTGGTC-3′) were used for amplification of hCPSF6-321. Primers BamHI hCPSF6 F (5′-AAGGATC CGCCACCATGGCGGACGGCGTGGACCAC-3′) and hCPSF6 375R stop NotI (5′-AATGCGGCCGCCTAGCTATCTGATGTAGGCATGC-3′) were used for amplification of hCPSF6-375. hCSPF6-358 and hCPSF6-412 were generated by site-directed mutagenesis using mCPSF6-358 and mCPSF6-412 on pCR2.1 as the templates, respectively, because our attempts to amplify the cDNA containing exon 6 in human cells were unsuccessful, and there exist only two amino acid substitutions at residues S153N and G192S in comparison with mCPSF6. Primers mCPSF6-S153N-5 (5′-GAACTTCATGGTCAGAATCCTGTTGTAACTCCA-3′) and mCPSF6-S153N-3 (5′-TGGAGTTACAACAGGATTCTGACCATG AAGTTC-3′) were used for S153N substitution. Primers mCPSF6-G192S-5 (5′-GGTCCTCCAGGAGGCAGTTCACGCGCAGCGTTT-3′) and mCPSF6-G192S-3 (5′-AAACGCTGCGCGTGAACTGCCTCCTGG AGGACC-3′) were used for G192S substitution. Full-length hCPSF6 was amplified by RT-PCR using as the template total RNA isolated from MOLT-4 human T cells by RNeasy minikit (Qiagen, Inc., Valencia, CA). Primers BamHI hCPSF6 F (5′-AAGGATCCGCCACCATGGCGGACGG CGTGGACCAC-3′) and hCPSF6 NotI (5′-AATGCGGCCGCCTAACGA TGACGATATTCGCGCTCTC-3′) were used. RT-PCR was performed with the PrimeScript II high-fidelity one-step RT-PCR kit (TaKaRa Bio, Inc., Shiga, Japan). The amplified PCR products were inserted into pCR2.1 and sequenced. The cDNA was inserted into the BamHI and NotI sites of pMRX-ires-puro (29). The resultant plasmids were referred to as pMRX-hCPSF6-321, pMRX-hCPSF6-358, pMRX-hCPSF6-375, pMRX-hCPSF6-412, and pMRX-hCPSF6, respectively.

Single-round infection assay. For infection of HEK293 cells, 3×10^5 cells were infected with 10 ng (p24) of VSV-G-pseudotyped NL4-3luc (VSV-G/NL4-3luc) (22) in 12-well plates, harvested, and lysed at 20 h postinfection. For infection of MT-4/CCR5 or MOLT-4 cells, 5×10^5 cells were infected with 10 ng (p24) of VSV-G/NL4-3luc in 24-well plates and harvested and lysed at 24 h postinfection. To compare the infectivities between VSV-G/NL4-3luc and VSV-G/NL4-3 CA N74D-luc, we used virus normalized with the RT count equivalent for 10 ng (p24) of VSV-G/NL4-3luc. To determine the luciferase activity, cell lysates were mixed with luciferase substrate and light emission was measured in a GloMAX multidetection system (Promega Corp, Madison, WI).

Fate-of-capsid assay. The fate-of-capsid assay was performed as previously described (13) with minor modifications. Approximately 5×10^6 HEK293 cells carrying the empty vector or those stably expressing hCPSF6-375, hCPSF6-412, or hemagglutinin-tagged mCPSF6-358 (mCPSF6-358-HA) were preplated in a 10-cm dish 1 day before the assay. Cells were inoculated with 5×10^6 RT counts of VSV-G/NL4-3luc at 4°C for 30 min, incubated at 37°C for 4 or 8 h, and then washed twice with ice-cold phosphate-buffered saline (PBS) containing 0.005% trypsin-EDTA to detach viruses from the cellular surface and once with ice-cold PBS to remove trypsin. Washed cells were resuspended in 1 ml of hypotonic lysis buffer (10 mM Tris-HCl [pH 8.0], 10 mM KCl, 1 mM EDTA, protease inhibitor cocktail [Nacalai Tesque, Inc., Kyoto, Japan]) and incubated on ice for 15 min. Swollen cells were lysed in a 7-ml Dounce homogenizer with a "tight" pestle (15 gentle strokes making a half-turn of pestle per each stroke), and cell lysates were cleared by centrifugation at $2{,}000 \times g$ for 3 min at 4°C. Fifty microliters of the cleared cell extract was collected as input. Cleared extracts (0.8 ml) were layered over 20% to 60% sucrose cushions prepared in PBS and centrifuged at 4°C at $115{,}000 \times g$ for 70 min in a Beckman SW50.1 rotor. Three fractions (1.1 ml each) were

collected from the top of the gradient. Aliquots of each fraction and input were subsequently subjected to immunoblotting.

Western blotting. Whole-cell lysates were prepared as follows. Cells were washed twice with PBS, suspended in radioimmunoprecipitation assay (RIPA) buffer (0.1% SDS, 25 mM Tris-HCl [pH 7.6], 150 mM NaCl, 1% NP-40, 1% sodium deoxycholate) (250 μl per 5 × 10^6 cells). The protein concentration was determined by Bradford assay, and the concentration was adjusted to 15 μg/15 μl with RIPA buffer. The lysate was mixed with an equal volume of 2× sample buffer (4% sodium dodecyl sulfate, 125 mM Tris-HCl [pH 6.8], 10% 2-mercaptoethanol, 10% glycerol, 0.002% bromophenol blue). Samples were subjected to SDS-PAGE, transferred to polyvinylidene difluoride (PVDF) membranes, and reacted with a rabbit polyclonal antibody to CPSF6 (Abcam, Inc., Cambridge, MA), a mouse monoclonal antibody to HIV-1 p24 (Abcam, Inc., Cambridge, MA), and a rabbit polyclonal antibody to β-actin (Abcam, Inc., Cambridge, MA). Membranes were then incubated with horseradish peroxidase-conjugated secondary antibody (Amersham Biosciences, Piscataway, NJ), and proteins were visualized by Western Lightning Plus-ECL (PerkinElmer, Waltham, MA) or enhanced chemiluminescence (Pierce Biotechnology, Rockford, IL).

Quantitation of viral cDNA. Prior to infection, virus solution was treated with 100 U of RNase-free DNase I (Roche Applied Science, Indianapolis, IN) in the presence of 10 mM $MgCl_2$ for 30 min at 37°C. For infection of HEK293 cells, 7 × 10^5 target cells were incubated for 6, 12, or 24 h with VSV-G/NL4-3luc virus supernatant containing 23 ng of p24. For infection of MT-4/CCR5 or MOLT-4 cells, 5 × 10^5 cells were incubated for 4, 8, or 24 h with an NL4-3 virus supernatant containing 50 ng of p24. Total cellular DNA was extracted using the DNeasy tissue kit (Qiagen, Inc., Valencia, CA). HIV-1 inactivated by incubation at 65°C for 30 min was used as a negative control. In real-time PCR, the primers U5-gag/F2 (5′-GTAGTGTGTGCCCGTCTGTTG-3′) (nt 553 to 573) and U5-gag/R2 (5′-CAAGCCGAGTCCTGCGT-3′) (nt 689 to 705) and probe U5-gag/probe2 (5′-FAM-TGGCGCCCGAACAGGGACTT-TAMRA-3′ [where FAM is 6-carboxyfluorescein and TAMRA is 6-carboxytetramethylrhodamine]) (nt 636 to 655) were used for amplification and quantitation of the U5-*gag* region of the HIV-1 late reverse transcription product (30). For standardization, the β-globin mRNA was quantitated as previously described (30). Real-time PCR was carried out with the StepOnePlus real-time PCR system (Applied Biosystems, Carlsbad, CA). The ratios of viral cDNA level to β-globin cDNA level are shown.

Analysis of HIV-1 replication in human T cells. MT-4/CCR5 cells (1 × 10^5) were exposed to HIV-1 supernatant containing 100 pg of p24. Virus production was monitored for 14 days postinfection by RT activity in the culture supernatants.

Establishment of HEK293, MOLT-4, and MT-4/CCR5 cells stably expressing the hCPSF6 mutant. HEK293, MOLT-4, and MT-4/CCR5 cells were transduced with retrovirus vector that confer puromycin resistance and express the hCPSF6 mutant. HEK293, MOLT-4, and MT-4/CCR5 cells stably expressing the hCPSF6 mutant were obtained after selection with 4 μg/ml puromycin for HEK293 and 2 μg/ml puromycin for MOLT-4 and MT-4/CCR5, respectively.

Depletion of hCPSF6 in HEK293 cells. HEK293 cells were transduced with HIV-1-based vectors that confer puromycin resistance and express either nontargeting short hairpin RNA (shRNA) or those targeting hCPSF6 (Sigma-Aldrich, Co., St. Louis, MO). Pools of HEK293 cells expressing shRNAs were established after selection with puromycin (4 μg/ml).

RESULTS

C-terminally truncated hCPSF6 identified in a functional screen. To identify proteins that interfere with HIV-1 infection by a functional screen using a cDNA expression library, we employed lethal selection with the herpes simplex virus thymidine kinase (HSV-TK) gene to exclude HIV-1-infected cells (Fig. 1A). HSV-TK is a typical suicide protein (31) that, in concert with cellular kinases, specifically converts the prodrug ganciclovir (GCV) into highly toxic GCV triphosphate, which causes DNA polymerase chain termination and eventual cell death. Previous reports showed that HSV-TK gene-carrying HIV-1 replication is inhibited by selective suicide of HIV-1-infected cells in the presence of GCV and is highly efficient in controlling spreading infection of HIV-1 in tissue culture (32). Thus, we generated HSV-TK gene-carrying HIV-1 by the insertion of the HSV-TK gene in pHIV-1_{NL4-3}-*env*(−) in place of the *nef* gene. Recombinant HIV-1 expressing HSV-TK and pseudotyped with the vesicular stomatitis virus G glycoprotein (denoted by HIV-1-TK) can efficiently infect cells of many mammalian species, including humans. We used a murine leukemia virus vector to express a human cDNA library prepared from human T-cell line MT-1 in HEK293 cells, which are highly susceptible to HIV-1-TK infection. After several rounds of HIV-1-TK infection at a high multiplicity of infection and subsequent GCV selection, we obtained and characterized surviving cell clones in terms of susceptibility to HIV infection, among which one clone was found to express a carboxy-terminally truncated fragment of human cleavage and polyadenylation factor 6 (hCPSF6-375).

We investigated if hCPSF6-375 affects HIV-1 infection in a manner similar to mCPSF6-358, which interferes with nuclear import of HIV. We established HEK293 cell pools stably expressing hCPSF6-375 or C-terminally hemagglutinin (HA)-tagged mCPSF6-358 (mCPSF6-358-HA), the latter of which was studied in the previous study (7). hCPSF6-375 was expressed at a level comparable to that of mCPSF6-358-HA, as verified by immunoblotting with an antibody to CPSF6 (Fig. 1B). As shown previously (7), mCPSF6-358-HA strongly inhibited infection with the single-round VSV-G-pseudotyped luciferase-carrying HIV-1 vector (VSV-G/NL4-3luc) (Fig. 1C). hCPSF6-375 also inhibited infection with VSV-G/NL4-3luc to a similar extent (Fig. 1C). Inhibition of HIV-1 infection was evident in HEK293 cells expressing hCPSF6-375 or mCPSF6-358-HA over a wide range of virus amounts (1 to 100 ng) in the HIV-1 p24 antigen (Fig. 1C).

To investigate the mechanism of inhibition, we measured the amount of viral cDNA synthesized after infection of target cells stably expressing either hCPSF6-375 or mCPSF6-358-HA (Fig. 1D). As reported previously (7), quantitative PCR revealed that the amount of the late reverse transcription product was not reduced in mCPSF6-358-HA-expressing cells (Fig. 1D). Interestingly, stable expression of hCPSF6-375 remarkably suppressed viral cDNA synthesis after HIV-1 infection (Fig. 1D). These results suggest that hCPSF6-375 and mCPSF6-358-HA have an inhibitory effect on HIV-1 infection, but have different modes of action at an early stage of HIV-1 infection. To further investigate whether the difference between hCPSF6-375 and mCPSF6-358-HA is due to their cellular localization or not, we fractionated cellular proteins into different compartments. As shown in Fig. 1E, hCPSF6-375 and mCPSF6-358-HA were predominantly localized in the cytoplasm, suggesting that the different actions of hCPSF6-375 and mCPSF6-358-HA on HIV-1 depend on their functional properties.

A previous report showed that the N74D HIV-1 capsid mutant is resistant to inhibition by mCPSF6-358-HA (7). We therefore examined if hCPSF6-375 inhibits N74D HIV-1 infection and found that hCPSF6-375 did not significantly affect infection with N74D HIV-1 (Fig. 1F). Collectively, hCPSF6-375 and mCPSF6-

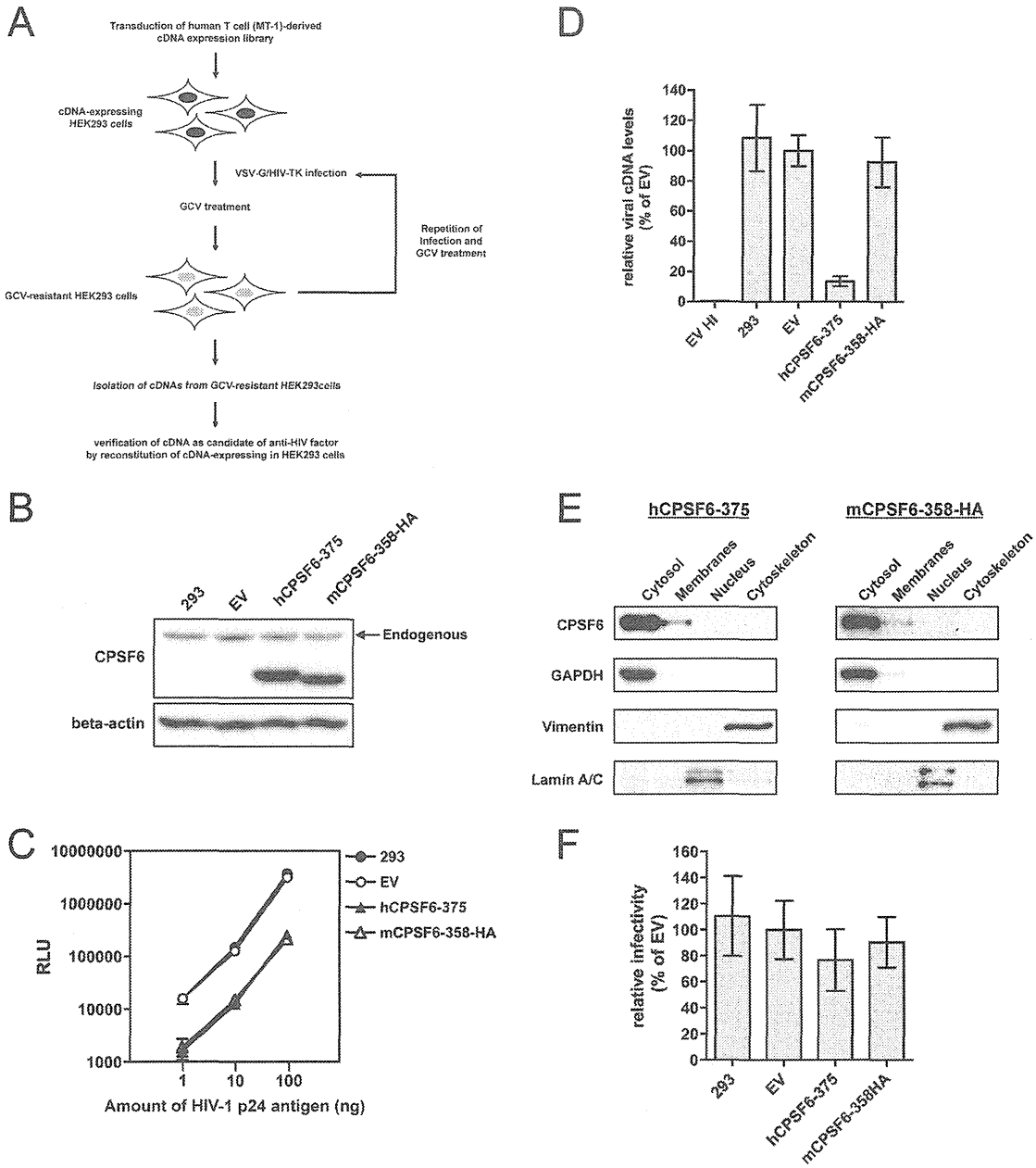

FIG 1 C-terminally truncated hCPSF6 identified in a functional screen inhibits virus cDNA synthesis. (A) HEK293 cells were transduced with VSV-G-pseudotyped retrovirus vector expressing a human T-cell-derived cDNA library. After a few passages, the cells were infected with high-titer HIV-1 capable of expressing HSV-TK (VSV-G/NL4-3TK) and subjected to lethal selection with ganciclovir (GCV) to eliminate infected cells. After repeated infection and selection, inserted cDNAs isolated from ganciclovir-resistant cells were amplified by PCR. The cDNAs were subcloned again in a retrovirus vector and expressed in HEK293 cells to verify the property as anti-HIV factor. (B) Immunoblot analysis of CPSF6 mutants. Lysates of HEK293 cells (293), control vector-infected HEK293 cells (EV control), and cells stably expressing hCPSF6-375 or mCPSF6-358-HA were subjected to immunoblot analysis with anti-CPSF6 or anti-β-actin antibodies. (C) Effect of CPSF6 mutants on viral infectivity. HEK293 cells stably expressing CPSF6 mutants were infected with VSV-G/NL4-3luc. Luciferase activity was measured 20 h after infection. The mean luciferase values in three independent experiments are shown. (D) Amount of viral cDNA synthesized after VSV-G/NL4-3luc infection. Total DNA was isolated from a portion of the cells 6 h after infection. Viral cDNA synthesis was quantified by real-time PCR as described in Materials and Methods. The mean value obtained from EV control cells was arbitrarily set as 100%. Mean values and standard deviations from three independent experiments are shown. (E) Localization of CPSF6 mutants in HEK293 cells. Cell lysates were prepared and separated by the Qproteome cell compartment kit (Qiagen, Inc., Valencia, CA). Fractions were subjected to immunoblot analysis with anti-CPSF6 antibody, anti-GAPDH antibody for the cytoplasmic fraction, antivimentin antibody for the cytoskeletal fraction, and anti-lamin A/C antibody for the nuclear fraction. (F) Effects of CPSF6 mutants on infection with HIV-1 carrying the N74D capsid mutation. HEK293 cells stably expressing CPSF6 mutants were infected with VSV-G/NL4-3 CA N74D-luc. Luciferase activity was measured 20 h after infection. The mean luciferase value from EV control cells was arbitrarily set as 100%.

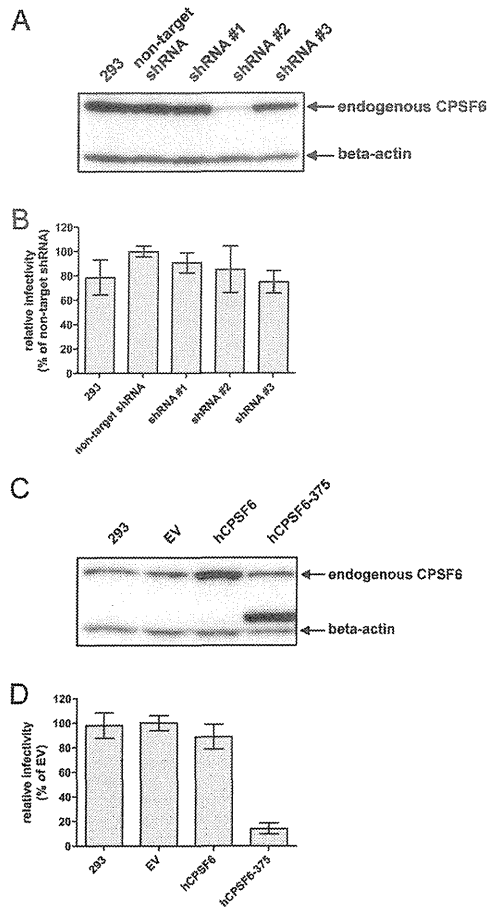

FIG 2 Involvement of full-length hCPSF6 in HIV-1 infection. (A) Immunoblot analysis of CPSF6 expression. Approximately 30 μg of whole-cell lysates from HEK293 cells stably expressing the indicated shRNAs was subjected to immunoblot analyses with anti-CPSF6 or anti-β-actin antibodies. (B) Effect of CPSF6 depletion on viral infectivity. HEK293 cells stably expressing the indicated shRNAs were infected with VSV-G/NL4-3luc. Luciferase activity was measured 20 h after infection. The mean luciferase value from control cells (nontarget shRNA) was arbitrarily set as 100%. (C) Immunoblot analysis of CPSF6 expression. Approximately 30 μg of whole-cell lysates from HEK293 control cells and those stably expressing full-length CPSF6 was subjected to immunoblot analyses with anti-CPSF6 or anti-β-actin antibodies. (D) Effect of full-length CPSF6 on viral infectivity. Experiments were done as described in panel B. The mean luciferase value from EV control cells was arbitrarily set as 100%.

358-HA appear to work against HIV-1 infection in the early phase of infection, though hCPSF6-375 inhibits viral cDNA synthesis.

To investigate if endogenous hCPSF6 is involved in HIV-1 infection, we depleted hCPSF6 in HEK293 cells (hCPSF6-KD). Lentivirus-mediated expression of an hCPSF6-specific shRNA, shRNA 2, successfully suppressed hCPSF6 expression (Fig. 2A). Depletion of hCPSF6 did not significantly alter the infectivity of VSV-G-pseudotyped NL4-3luc, suggesting that hCPSF6 is not a cofactor required for HIV-1 infection (Fig. 2B, compare the lanes containing nontarget shRNA and shRNA 2). We next investigated if elevated expression of full-length human CPSF6 impairs HIV-1 infection. As shown in Fig. 2C and D, stable expression of ectopic human CPSF6 had little effect on HIV-1 infection, suggesting that full-length CPSF6 by itself does not work as a restriction factor on HIV-1.

Lack of exon 6-encoded polypeptide in hCPSF6-375 is responsible for impaired viral cDNA synthesis. To explore the determinant responsible for viral cDNA synthesis inhibition, we compared amino acid sequences of hCPSF6-375 and mCPSF6-358 (Fig. 3A). We found in hCPSF6-375 two amino acid substitutions at residues N153S and S192G, a deletion of amino acids encoded by exon 6 (residues 232 to 268 in mouse CPSF6 and denoted by "Ex6"), and addition of the C-terminal 54 residues (Fig. 3A). We therefore generated two mCPSF6-based mutants with humanized amino acid substitutions S153N and G192S in mCPSF6-358 (hCPSF6-358) and in mCPSF6-412 (hCPSF6-412) (Fig. 3B). We also generated hCPSF6-321 based on hCPSF6-375 (Fig. 3B). Each mutant was assayed for stable expression in HEK293 cells after retrovirus vector transduction and antibiotic selection.

We first investigated a possible effect of two amino acid substitutions between hCPSF6-358 and mCPSF6-358 on the inhibition of HIV-1 infection. hCPSF6-358 was expressed at a level comparable to that of mCPSF6-358 (Fig. 3C, compare hCPSF6-358 and mCPSF6-358). Infection efficiency was determined by either a standard luciferase assay (Fig. 3D) or by quantitative PCR (Fig. 3E). Untagged mCPSF6-358 as well as mCPSF6-358-HA strongly inhibited infection with VSV-G/NL4-3luc despite lower expression of untagged mCPSF6-358 (Fig. 3C and D, compare mCPSF6-358 and mCPSF6-358-HA). hCPSF6-358 also inhibited infection by VSV-G/NL4-3luc (Fig. 3D, hCPSF6-358). Like mCPSF6-358-HA, the amount of viral cDNA synthesized after HIV-1 infection of hCPSF6-358-expressing cells was not reduced (Fig. 3E, hCPSF6-358). Moreover, untagged and C-terminally HA-tagged mCPSF6-358 had little effect on viral cDNA synthesis after HIV-1 infection (Fig. 3E, compare mCPSF6-358 and mCPSF6-358-HA). These results suggest that the C-terminal HA tag or two-amino-acid difference between hCPSF6-358 and mCPSF6-358 does not apparently alter the inhibitory property of mCPSF6-358-HA. Furthermore, we also generated mouse CPSF6-375 to investigate possible effects of the two amino acid substitutions between hCPSF6-375 and mCPSF6-375 on the inhibition of HIV-1 infection. As shown in Fig. 3F to H, the effects of mCPSF6-375 on HIV-1 inhibition were similar to those of hCPSF6-375, indicating that the two amino acid substitutions do not significantly alter the inhibitory properties, even in the context of CPSF6-375 (Fig. 3G and H, compare hCPSF6-375 and mCPSF6-375).

To assess the contribution of Ex6 in hCPSF6-358 to the inhibition of HIV-1 infection, we used Ex6-deficient hCPSF6-321. hCPSF6-321 was expressed at a level comparable to that of hCPSF6-358, and the HIV-1 infectivity in hCPSF6-321-expressing cells determined by luciferase assay was comparable to that hCPSF6-358-expressing cells (Fig. 3C and D, compare hCPSF6-321 and hCPSF6-358). Importantly, viral cDNA synthesis after HIV-1 infection in hCPSF6-321-expressing cells was dramatically suppressed in comparison with that in hCPSF6-358-expressing cells (Fig. 3E, compare hCPSF6-321 and hCPSF6-358). On the other hand, addition of Ex6 to hCPSF6-375 (hCPSF6-412) substantially attenuated the inhibition of viral DNA synthesis (Fig. 3E, compare hCPSF6-375 and hCPSF6-412). These results suggest that CPSF6 mutants with Ex6 do not inhibit viral cDNA synthesis.

We also assessed the contribution of the C-terminal 54 residues of hCPSF6-375, which are absent from hCPSF6-321, to the inhibition of HIV-1 infection. hCPSF6-321, when expressed at a level comparable to that of hCPSF6-375, achieved similar inhibition of

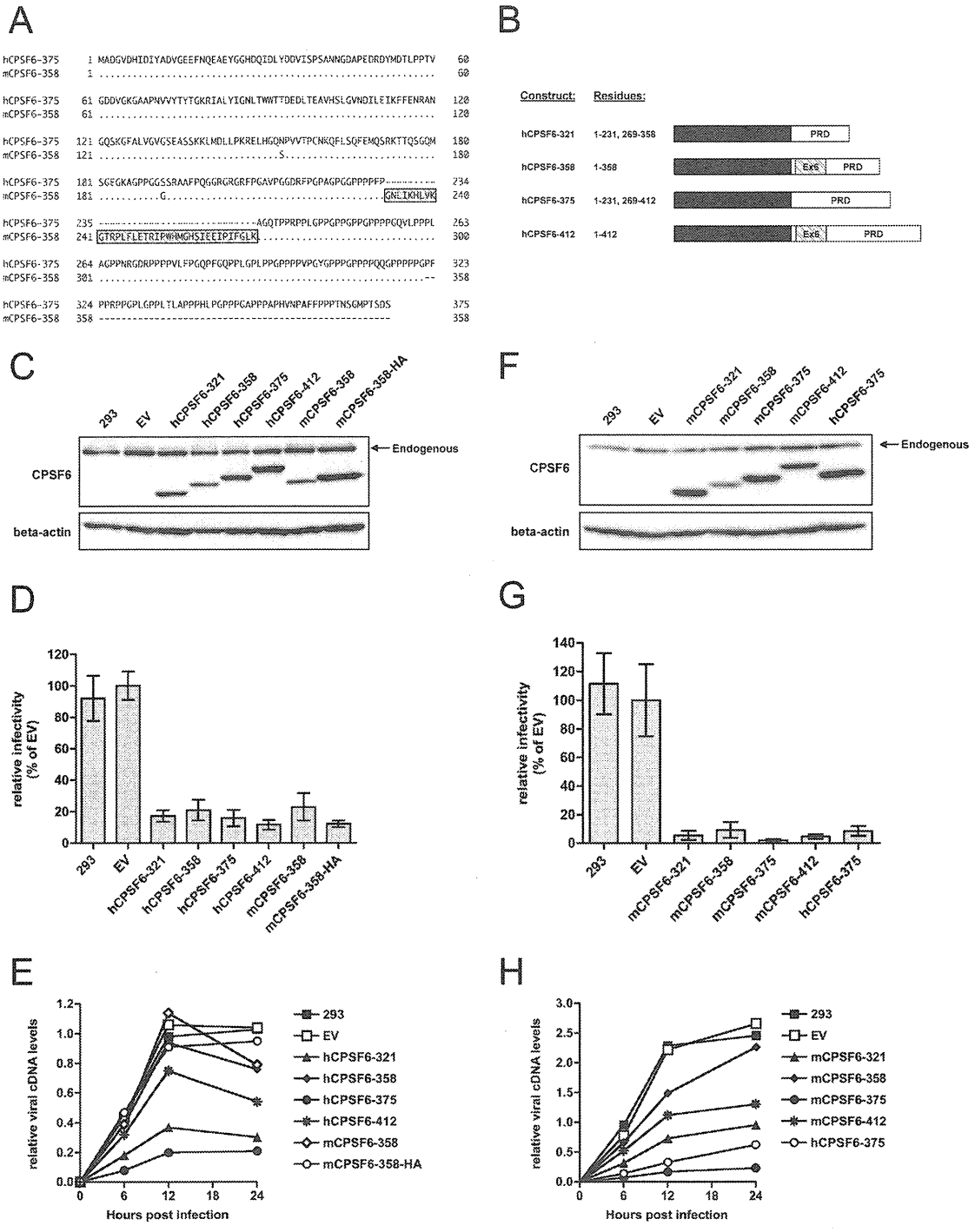

FIG 3 Effects of Ex6 deletion on HIV-1 infection. (A) Amino acid alignments of hCPSF6-375 and mCPSF6-358. Dots indicate sequence identity, and dashes indicate gap introduction to preserve alignment. Amino acids in the reticulate area indicate the region of exon 6. (B) Schematic presentation of hCPSF6 mutants. "Ex6" in the reticulate area indicates the domain encoded by exon 6, and "PRD" represents the proline-rich domain. (C) Immunoblot analysis of HEK293 cells expressing truncated forms of hCPSF6. Approximately 30 μg of whole-cell lysates was subjected to immunoblot analyses using anti-CPSF6 or anti-β-actin antibodies. (D) Effect of hCPSF6 mutants on viral infectivity. HEK293 cells stably expressing hCPSF6 mutants were infected with VSV-G/NL4-3luc. Luciferase activity was measured 20 h after infection. The mean luciferase value from EV control cells was arbitrarily set as 100%. (E) Kinetics of viral cDNA synthesis *in vivo*. Total DNA was isolated from a portion of the cells at the indicated times after infection. Viral cDNA synthesis was quantified by real-time PCR as described in Materials and Methods. Mean values in three independent experiments are shown. (F) Immunoblot analysis of mouse CPSF6 mutants expressed in HEK293 cells. Experiments were done as described in panel C. (G) Effect of mCPSF6 mutants on viral infectivity. Experiments were done as described in panel D. (H) Kinetics of viral cDNA synthesis *in vivo*. Experiments were done as described in panel E.

VSV-G/NL4-3luc infection (Fig. 3C and D, compare hCPSF6-321 and hCPSF6-375). The fact that hCPSF6-321 potently suppresses viral cDNA synthesis also suggests that the C-terminal 54 residues in hCPSF6-375 are not essentially required for viral cDNA synthesis inhibition (Fig. 3E, compare hCPSF6-321 and hCPSF6-375). Collectively, these results indicate that the absence of Ex6, but not the C-terminal 54 residues in hCPSF6-375, is responsible for viral cDNA synthesis inhibition.

CPSF6-375 alters the kinetics of HIV-1 capsid disassembly. Previous reports showed that optimal dissociation of capsid from the HIV-1 core is required for efficient viral cDNA synthesis in target cells (17–19). To investigate the effect of hCPSF6-375 on the stability of the HIV-1 core after HIV-1 entry, we performed the fate-of-the-capsid assay as described previously (13). Previous studies showed that step gradient analyses could distinguish soluble from core-associated HIV-1 proteins (33–36). To clearly separate HIV-1 cores from the soluble capsid protein after HIV-1 entry into target cells, we employed 20% and 60% sucrose cushions for ultracentrifugation, where the HIV-1 core is expected to be enriched at the border of 20% and 60% cushions. Our modified assay is summarized in Fig. 4A. HIV-1 soluble capsid partitions to fraction a, while the integrated HIV-1 core accumulates in fraction c. A buffer fraction (Fig. 4A, fraction b) was set to separate the fractions a and c (Fig. 4, fractions a and c). This assay was applied to examine the fate of the HIV-1 capsid after infection of HEK293 cells expressing hCPSF6-375 or mCPSF6-375-HA and control cells transduced with the empty retrovirus vector (EV). We also used NL4-3 virions without any envelope protein (Env^-) as the HIV-1 entry control (13). The virions were allowed to attach to the target cells for 30 min at 4°C, and then the temperature was shifted to 37°C to initiate infection. At 4 or 8 h after temperature shifting, the cells were lysed and the cell lysates analyzed by step gradient centrifugation. The amounts of p24 capsid protein in the cell lysate were similar in hCPSF6-375, mCPSF6-358-HA, and EV control cells (Fig. 4B, input), and p24 capsid protein was not detected in cell lysate derived from EV control cells incubated with the HIV-1 (Env^-) virions, indicating that this assay can correctly measure HIV-1 capsid protein in the cytosol of target cells after HIV-1 infection (Fig. 4B, compare EV-Env^- and EV-Env^+).

Immunoblot analyses revealed that the amount of HIV-1 cores in HIV-1-infected cells expressing hCPSF6-375 was smaller than those detected in mCPSF6-358-HA or control EV cells at 4 (Fig. 4B, upper panel) and 8 h (Fig. 4B, lower panel) post-temperature shifting (Fig. 4B, fraction c, compare hCPSF6-375 and mCPSF6-358-HA). This was further confirmed quantitatively by p24 ELISA of each fraction (Fig. 4B). The levels of p24 capsid protein in the cell lysates from control cells or those expressing CPSF6 mutants were comparable (Fig. 4C, input). In contrast, the amount of particulate HIV-1 capsid in cells expressing hCPSF6-375 was obviously decreased at all time points examined (Fig. 4C, fraction c). No p24 capsid protein was detected in fractions lower than fraction c or pellets prepared from cells exposed to VSV-G/NL4-3luc or NL4-3luc (Env^-) virions, indicating that the particulate HIV-1 capsid accumulates only in fraction c (data not shown). These data indicate that the presence of hCPSF6-375 in target cells accelerates HIV-1 capsid disassembly in newly infected cells.

CPSF6-375 inhibits HIV-1 replication in human T cells. To see if the inhibitory effects of hCPSF6-375 on HIV-1 infection are cell type specific or not limited to HEK293 cells, similar experiments were performed with MOLT-4 human T-cell lines. We made use of MOLT-4 cells expressing hCPSF6-321, -358, -375, or -412 or mCPSF6-358-HA and control cells transduced with EV. The presence of comparable amounts of hCPSF6 mutants except hCPSF6-358 was verified by immunoblotting using a CPSF6-specific antibody (Fig. 5A). mCPSF6-358-HA was expressed at a level comparable to that of hCPSF6-375 (Fig. 5A, compare hCPSF6-375 and mCPSF6-358-HA). The effect of hCPSF6 mutants on the infectivity of MOLT-4 cells was analyzed in a single-round infectivity assay with VSV-G/NL4-3luc. As expected, hCPSF6-375 strongly inhibited HIV-1 infection (Fig. 5B, compare EV and hCPSF6-375). Similarly, mCPSF6-358-HA as well as hCPSF6-358 also inhibited infection with VSV-G/NL4-3luc (Fig. 5B, compare hCPSF6-358 and mCPSF6-358-HA).

How each mutant affects viral cDNA synthesis was determined by measuring the amount of the late reverse transcription product in target cells stably expressing hCPSF6-375 mutants or mCPSF6-358-HA after HIV-1 infection (Fig. 5C). Similar results shown in Fig. 3E were obtained by quantitative PCR indicating that hCPSF6-375 but not mCPSF6-358-HA inhibited viral cDNA synthesis after HIV-1 infection, suggesting that the inhibitory effect of hCPSF6-375 on HIV-1 DNA synthesis is not cell type specific (Fig. 5C, compare hCPSF6-375 and mCPSF6-358-HA).

A recent study showed that mCPSF6-358 inhibits spreading infection with HIV-1 in a human T-lymphoid cell line (7). To further investigate the effect of hCPSF6-375 on spreading infection with HIV-1 in human T cells, we established MT-4/CCR5 human T-cell lines stably expressing hCPSF6-375 and mCPSF6-358-HA (Fig. 5D). The effect of hCPSF6-375 on the infectivity of MT-4/CCR5 cells was first analyzed in a single-round infectivity assay. Consistent with the results shown in Fig. 3D and 5B, both hCPSF6-375 and mCPSF6-358-HA strongly inhibited infection with VSV-G/NL4-3luc (Fig. 5E). These results provide additional evidence that the inhibitory effect of hCPSF6-375 on HIV-1 infection is not cell type specific. We next investigated the effect of hCPSF6-375 on HIV-1 replication in MT-4/CCR5 T cells with the replication-competent NL4-3 virus. Control EV cells well supported HIV-1 replication, with a peak of RT activity on day 6, while HIV-1 replication was inhibited by mCPSF6-358-HA, as reported previously (7). hCPSF6-375 suppressed HIV-1 replication as potently as mCPSF6-358-HA in MT-4/CCR5 T cells (Fig. 5F).

DISCUSSION

In this study, we established an expression cloning system coupled with selective killing of HIV-1-infected cells to isolate anti-HIV-1 factors and obtained a C-terminally truncated CPSF6 protein, hCPSF6-375, which inhibited HIV-1 at an early stage of infection. Lee et al. previously screened a mouse cDNA library and identified mCPSF6-358, showing that it did not affect reverse transcription but inhibited HIV-1 trafficking to the nucleus (7). A notable difference from mCPSF6-358 is the absence of Ex6 in hCPSF6-375.

Our results revealed that both hCPSF6-375 and mCPSF6-358-HA inhibited infection by the single-round VSV-G/NL4-3luc infection (Fig. 1C). One remarkable finding of the present study is that hCPSF6-375 inhibited HIV-1 infection at the reverse transcription stage, suggesting a different mode of action in the early phase of HIV-1 infection in comparison with mCPSF6-358-HA (Fig. 1D). The localization of hCPSF6-375 as well as mCPSF6-358-HA was predominantly cytoplasmic (Fig. 1E), while endogenous hCPSF6 is normally enriched in the nucleus (37), and the

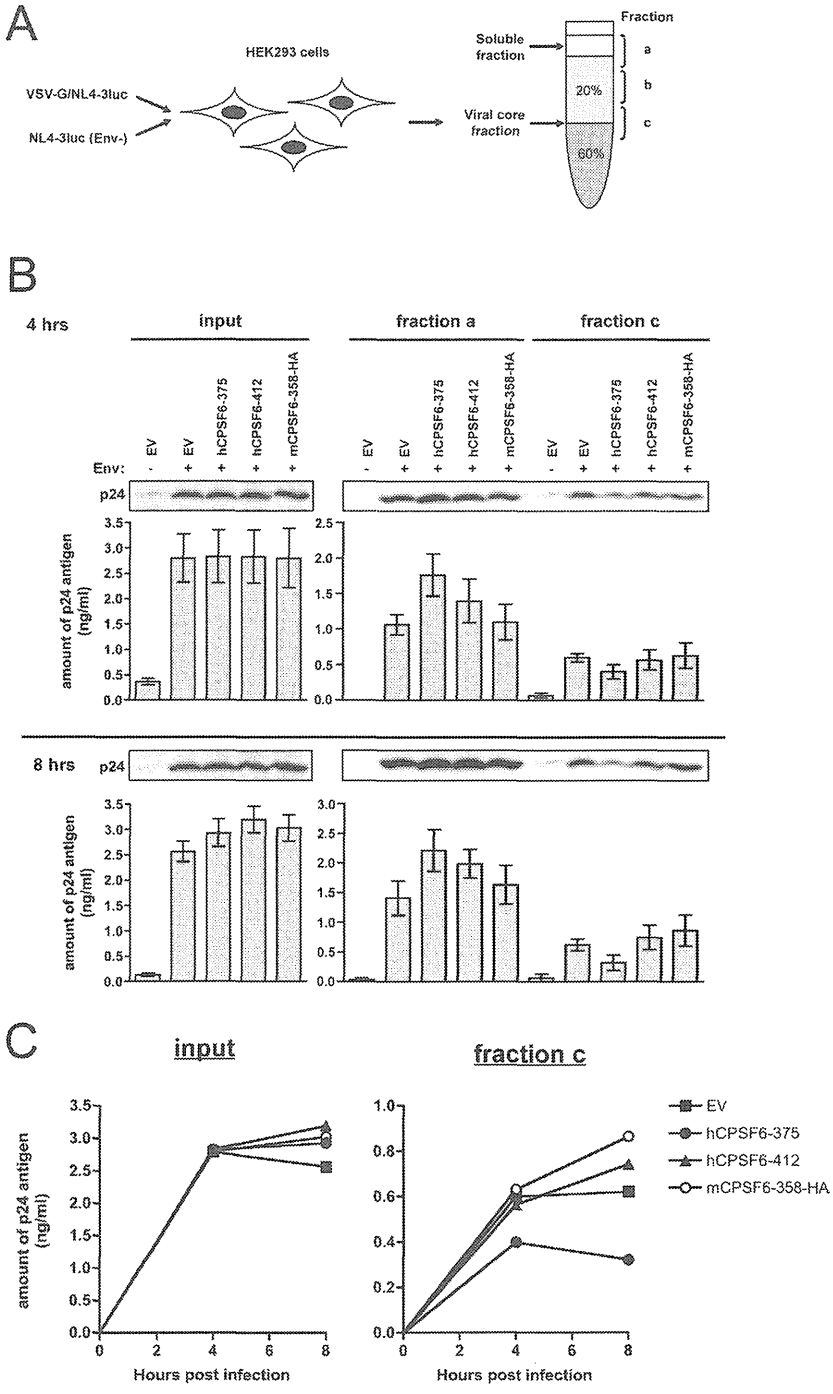

FIG 4 Deletion of Ex6 facilitates HIV-1 capsid disassembly. (A) Schematic diagram of the fate-of-capsid assay. HEK293 cells expressing CPSF6 mutants or the empty control vector (EV) were incubated with VSV-G/NL4-3luc or NL4-3luc (Env^-) at 4°C for 30 min and then at 37°C for the indicated times. Cell lysates were prepared and analyzed on the step gradient (20%/60%) of sucrose as described in Materials and Methods. (B) Aliquots of each fraction were processed for immunoblotting with anti-HIV-1 p24 antibodies. Representative results of a single experiment are shown. The accumulation of viral protein in each fraction was quantified by HIV-1 CA (p24) enzyme-linked immunosorbent assay, and mean values and standard deviations from three independent experiments are shown. (C) Graphic presentation of p24 capsid protein levels measured by p24 ELISA in the whole-cell lysate (left panel, input) or the viral core fraction (right panel, fraction c) at the indicated times shown in panel B. Mean values from three independent experiments are shown.

different actions of hCPSF6-375 and mCPSF6-358-HA on HIV-1 cannot be explained by the protein expression levels (Fig. 1B, compare hCPSF6-375 and mCPSF6-358-HA). Consistent with the previous report (7), elevated expression of full-length human CPSF6 and depletion of endogenous hCPSF6 had little effect on HIV-1 infection in our present study (Fig. 2), suggesting unique anti-HIV-1 properties of these truncated proteins. We initially attempted to compare hCPSF6-375 and untagged mCPSF6-358 in

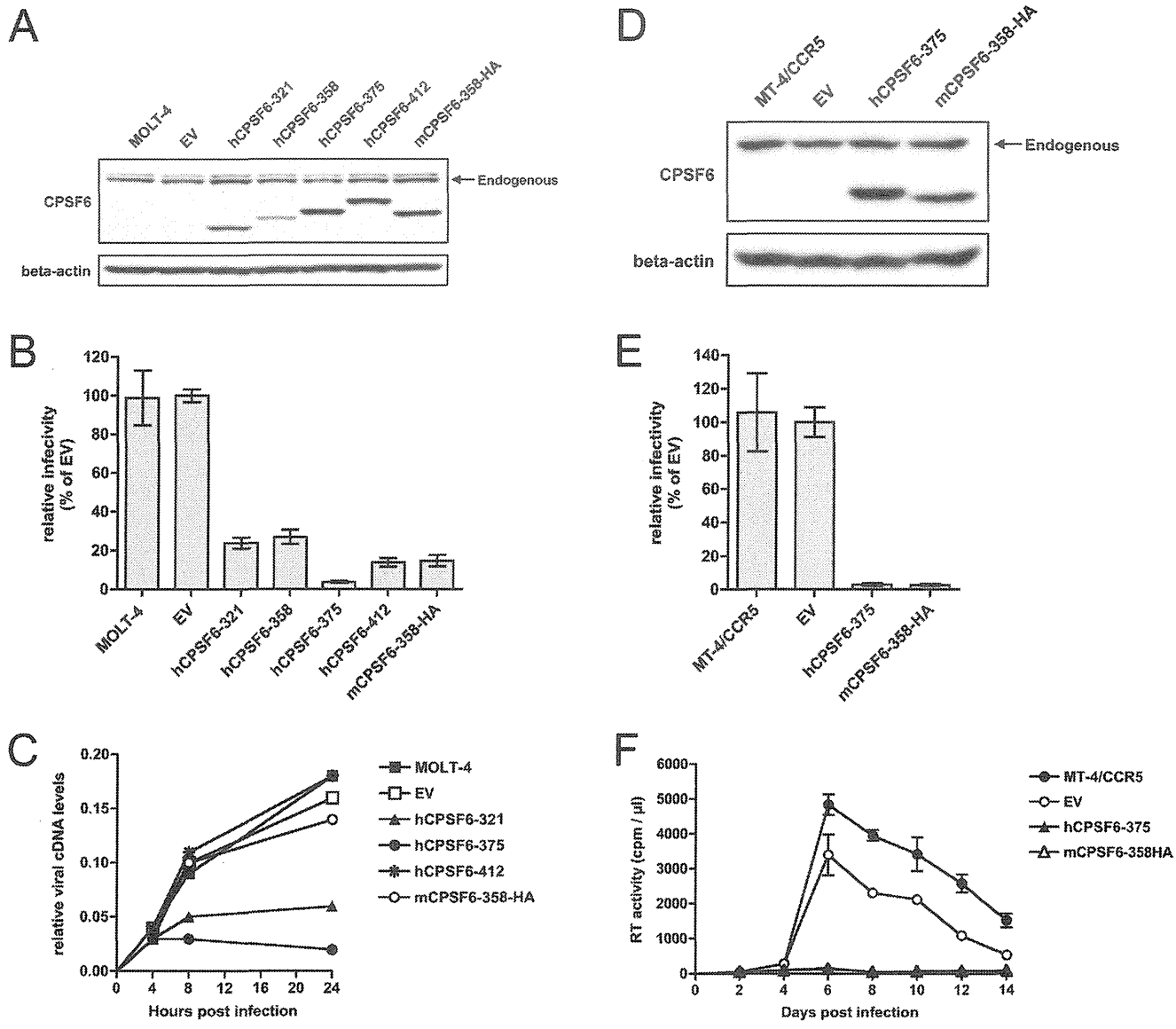

FIG 5 Effects of Ex6 deletion on HIV-1 replication in human T cells. (A) Immunoblot analysis of CPSF6 mutants expressed in MOLT-4 human T cells. Approximately 30 µg of whole-cell lysates was subjected to immunoblot analyses with anti-CPSF6 or anti-β-actin antibodies. (B) Effect of CPSF6 mutants on viral infectivity. MOLT-4 cells stably expressing CPSF6 mutants were infected with VSV-G/NL4-3luc. Luciferase activity was measured 24 h after infection. The mean luciferase value from EV control cells was arbitrarily set as 100%. (C) Kinetics of viral cDNA synthesis *in vivo*. Total DNA was isolated from a portion of the cells at the indicated times after infection. Viral cDNA synthesis was quantified by real-time PCR as described in Materials and Methods. Mean values in three independent experiments are shown. (D) Immunoblot analysis of hCPSF6-375 and mCPSF6-358-HA expressed in MT-4/CCR5 human T cells. Experiments were done as described in panel A. (E) Effect of CPSF6 mutants on viral infectivity in MT-4/CCR5 cells. Experiments were done as described in panel B. (F) CPSF6 mutants suppress spreading infection of HIV-1. Virus production in parental, EV control, hCPSF6-375-expressing, and mCPSF6-358-HA-expressing MT-4/CCR5 cells was monitored for 14 days by measuring the virus-associated reverse transcriptase activity in the culture supernatants. Mean values and standard deviations from three independent experiments are shown.

terms of HIV-1 restriction, but the stable expression level of mCPSF6-358 was much lower than that of hCPSF6-375 (Fig. 3C, compare hCPSF6-375 and mCPSF6-358). We therefore investigated the effect of mCPSF6-358 on HIV-1 infection in the presence or absence of HA tag (Fig. 3D and E). Both untagged and HA-tagged mCPSF6-358 inhibited HIV-1 infection, as determined with VSV-G/NL4-3luc, despite lower expression of untagged mCPSF6-358 (Fig. 3C and D, compare mCPSF6-358 and mCPSF6-358-HA). Untagged and C-terminally HA-tagged mCPSF6-358 had little effect on viral cDNA synthesis after HIV-1 infection (Fig. 3E, compare mCPSF6-358 and mCPSF6-358-HA). On the basis of the results shown in Fig. 3C to E, we decided to use C-terminally HA-tagged mCPSF6 (mCPSF6-358-HA) to compare the anti-HIV-1 effects with those of hCPSF6-375. A previous study showed that N74D capsid mutation in HIV-1 led to HIV-1 resistance to mCPSF6-358 (7). We found that the N74D mutant is also resistant to hCPSF6-375, suggesting that hCPSF6-375 inhibition of HIV-1 also relies on the capsid sequence.

We have provided evidence that lack of Ex6 in C-terminally truncated forms of hCPSF6 is responsible for the inhibition of

viral cDNA synthesis after HIV-1 infection (Fig. 1D, 3E, and 5C). Lee et al. showed that mCPSF6-358 residues 301 to 358 are sufficient for inhibition of HIV-1 and minimal residues 313 to 327 contribute to anti-HIV-1 activity (11). The residues 313 to 327 are located downstream of Ex6 in CPSF6-358 and conserved in all hCPSF6 mutants used in this study. hCPSF6-321, the Ex6-deficient form of hCPSF6-358 inhibited HIV-1 infection at a level comparable to that of hCPSF6-358 in a single-round infectivity assay with VSV-G/NL4-3luc (Fig. 3D and 5B, compare hCPSF6-321 and hCPSF6-358). Similar results were obtained when hCPSF6-375 was compared with hCPSF6-412 (Fig. 3D and 5B, compare hCPSF6-375 and hCPSF6-412). These results indicate that Ex6 of CPSF6 is not essentially involved in HIV-1 inhibition.

We tried the fate-of-capsid assay with minor modifications, and our observation that the amount of HIV-1 cores in hCPSF6-375-expressing cells was lower than those detected in control, mCPSF6-358-HA, and hCPSF6-412 cells implies that the presence of hCPSF6-375 in target cells accelerated disassembly of HIV-1 capsid (Fig. 4B and C). A previous report showed that mCPSF6-358 could bind to tubular complexes composed of the HIV-1 capsid protein, suggesting physical interaction between particulate capsid and mCPSF6-358 (7). It is therefore conceivable that mCPSF6-358 binds to particulate capsid after HIV-1 infection, but does not alter the disassembly kinetics of capsid, having no detectable effect on viral cDNA synthesis. Our findings that hCPSF6-375 blocks HIV-1 infection by impairing both the viral cDNA synthesis and optimal stability of the HIV-1 core in target cells are reminiscent of the activity of restriction factors such as TRIM5α (13, 38). A previous study showed that a peptide corresponding to CPSF6 residues 313 to 327 was sufficient for direct binding to HIV-1 capsid (12). Since the CPSF6 residues 313 to 327 are conserved in all hCPSF6-375 mutants mentioned above, it is plausible that the polypeptide encoded by exon 6 of human CPSF6 influences the mode of interaction between HIV-1 capsid and hCPSF6, eventually giving a different outcome. The precise mechanism of the rapid disassembly of HIV-1 capsid in the presence of hCPSF6-375 in target cells remains to be further investigated.

In conclusion, the present study has clearly demonstrated that C-terminally truncated forms of CPSF6, when deleted with exon 6, promote capsid disassembly and interfere with viral reverse transcription, although the mechanism of actions remain to be determined. Elucidation of the mechanism(s) of inhibition of HIV-1 by hCPSF6 mutants could provide new insights for understanding viral cDNA synthesis in light of viral capsid disassembly.

ACKNOWLEDGMENTS

We thank I. S. Chen for providing pNL4-3luc (*env nef* mutant).

This work was supported by grant 21390136 from the Ministry of Education, Culture, Sports, Science, and Technology to S.Y. and by grant H22-AIDS-007 for Young Scientists of HIV/AIDS Research from the Ministry of Health, Labor, and Welfare of Japan to H.T.

REFERENCES

1. **Goff SP.** 2007. Host factors exploited by retroviruses. Nat. Rev. Microbiol. 5:253–263.
2. **Freed EO.** 2004. HIV-1 and the host cell: an intimate association. Trends Microbiol. 12:170–177.
3. **Brass AL, Dykxhoorn DM, Benita Y, Yan N, Engelman A, Xavier RJ, Lieberman J, Elledge SJ.** 2008. Identification of host proteins required for HIV infection through a functional genomic screen. Science 319:921–926.
4. **Konig R, Zhou Y, Elleder D, Diamond TL, Bonamy GM, Irelan JT, Chiang CY, Tu BP, De Jesus PD, Lilley CE, Seidel S, Opaluch AM, Caldwell JS, Weitzman MD, Kuhen KL, Bandyopadhyay S, Ideker T, Orth AP, Miraglia LJ, Bushman FD, Young JA, Chanda SK.** 2008. Global analysis of host-pathogen interactions that regulate early-stage HIV-1 replication. Cell 135:49–60.
5. **Zhou H, Xu M, Huang Q, Gates AT, Zhang XD, Castle JC, Stec E, Ferrer M, Strulovici B, Hazuda DJ, Espeseth AS.** 2008. Genome-scale RNAi screen for host factors required for HIV replication. Cell Host Microbe 4:495–504.
6. **Kawano Y, Yoshida T, Hieda K, Aoki J, Miyoshi H, Koyanagi Y.** 2004. A lentiviral cDNA library employing lambda recombination used to clone an inhibitor of human immunodeficiency virus type 1-induced cell death. J. Virol. 78:11352–11359.
7. **Lee K, Ambrose Z, Martin TD, Oztop I, Mulky A, Julias JG, Vandegraaff N, Baumann JG, Wang R, Yuen W, Takemura T, Shelton K, Taniuchi I, Li Y, Sodroski J, Littman DR, Coffin JM, Hughes SH, Unutmaz D, Engelman A, KewalRamani VN.** 2010. Flexible use of nuclear import pathways by HIV-1. Cell Host Microbe 7:221–233.
8. **Urano E, Kariya Y, Futahashi Y, Ichikawa R, Hamatake M, Fukazawa H, Morikawa Y, Yoshida T, Koyanagi Y, Yamamoto N, Komano J.** 2008. Identification of the P-TEFb complex-interacting domain of Brd4 as an inhibitor of HIV-1 replication by functional cDNA library screening in MT-4 cells. FEBS Lett. 582:4053–4058.
9. **Valente ST, Gilmartin GM, Mott C, Falkard B, Goff SP.** 2009. Inhibition of HIV-1 replication by eIF3f. Proc. Natl. Acad. Sci. U. S. A. 106:4071–4078.
10. **Valente ST, Goff SP.** 2006. Inhibition of HIV-1 gene expression by a fragment of hnRNP U. Mol. Cell 23:597–605.
11. **Lee K, Mulky A, Yuen W, Martin TD, Meyerson NR, Choi L, Yu H, Sawyer SL, Kewalramani VN.** 2012. HIV-1 capsid-targeting domain of cleavage and polyadenylation specificity factor 6. J. Virol. 86:3851–3860.
12. **Price AJ, Fletcher AJ, Schaller T, Elliott T, Lee K, KewalRamani VN, Chin JW, Towers GJ, James LC.** 2012. CPSF6 defines a conserved capsid interface that modulates HIV-1 replication. PLoS Pathog. 8:e1002896. doi:10.1371/journal.ppat.1002896.
13. **Stremlau M, Perron M, Lee M, Li Y, Song B, Javanbakht H, Diaz-Griffero F, Anderson DJ, Sundquist WI, Sodroski J.** 2006. Specific recognition and accelerated uncoating of retroviral capsids by the TRIM5alpha restriction factor. Proc. Natl. Acad. Sci. U. S. A. 103:5514–5519.
14. **Briones MS, Dobard CW, Chow SA.** 2010. Role of human immunodeficiency virus type 1 integrase in uncoating of the viral core. J. Virol. 84:5181–5190.
15. **Forshey BM, Aiken C.** 2003. Disassembly of human immunodeficiency virus type 1 cores in vitro reveals association of Nef with the subviral ribonucleoprotein complex. J. Virol. 77:4409–4414.
16. **Ohagen A, Gabuzda D.** 2000. Role of Vif in stability of the human immunodeficiency virus type 1 core. J. Virol. 74:11055–11066.
17. **Forshey BM, von Schwedler U, Sundquist WI, Aiken C.** 2002. Formation of a human immunodeficiency virus type 1 core of optimal stability is crucial for viral replication. J. Virol. 76:5667–5677.
18. **Leschonsky B, Ludwig C, Bieler K, Wagner R.** 2007. Capsid stability and replication of human immunodeficiency virus type 1 are influenced critically by charge and size of Gag residue 183. J. Gen. Virol. 88:207–216.
19. **Tang S, Murakami T, Agresta BE, Campbell S, Freed EO, Levin JG.** 2001. Human immunodeficiency virus type 1 N-terminal capsid mutants that exhibit aberrant core morphology and are blocked in initiation of reverse transcription in infected cells. J. Virol. 75:9357–9366.
20. **von Schwedler UK, Stray KM, Garrus JE, Sundquist WI.** 2003. Functional surfaces of the human immunodeficiency virus type 1 capsid protein. J. Virol. 77:5439–5450.
21. **Morita S, Kojima T, Kitamura T.** 2000. Plat-E: an efficient and stable system for transient packaging of retroviruses. Gene Ther. 7:1063–1066.
22. **Planelles V, Bachelerie F, Jowett JB, Haislip A, Xie Y, Banooni P, Masuda T, Chen IS.** 1995. Fate of the human immunodeficiency virus type 1 provirus in infected cells: a role for *vpr*. J. Virol. 69:5883–5889.
23. **Takeuchi H, Ishii H, Kuwano T, Inagaki N, Akari H, Matano T.** 2012. Host cell species-specific effect of cyclosporine A on simian immunodeficiency virus replication. Retrovirology 9:3. doi:10.1186/1742-4690-9-3.
24. **Willey RL, Smith DH, Lasky LA, Theodore TS, Earl PL, Moss B, Capon DJ, Martin MA.** 1988. In vitro mutagenesis identifies a region within the envelope gene of the human immunodeficiency virus that is critical for infectivity. J. Virol. 62:139–147.
25. **Tulin EE, Onoda N, Maeda M, Hasegawa M, Nosaka T, Nomura H,**

Asano S, Kitamura T. 2001. A novel secreted form of immune suppressor factor with high homology to vacuolar ATPases identified by a forward genetic approach of functional screening based on cell proliferation. J. Biol. Chem. 276:27519–27526.
26. **Saitoh T, Nakayama M, Nakano H, Yagita H, Yamamoto N, Yamaoka S.** 2003. TWEAK induces NF-kappaB2 p100 processing and long lasting NF-kappaB activation. J. Biol. Chem. 278:36005–36012.
27. **Saitoh Y, Yamamoto N, Dewan MZ, Sugimoto H, Martinez Bruyn VJ, Iwasaki Y, Matsubara K, Qi X, Saitoh T, Imoto I, Inazawa J, Utsunomiya A, Watanabe T, Masuda T, Yamaoka S.** 2008. Overexpressed NF-kappaB-inducing kinase contributes to the tumorigenesis of adult T-cell leukemia and Hodgkin Reed-Sternberg cells. Blood 111:5118–5129.
28. **Chinanonwait N, Miura H, Yamamoto N, Yamaoka S.** 2002. A recessive mutant cell line with a constitutive IkappaB kinase activity. FEBS Lett. 531:553–560.
29. **Saitoh T, Nakano H, Yamamoto N, Yamaoka S.** 2002. Lymphotoxin-beta receptor mediates NEMO-independent NF-kappaB activation. FEBS Lett. 532:45–51.
30. **Feng WY, Tanaka R, Inagaki Y, Saitoh Y, Chang MO, Amet T, Yamamoto N, Yamaoka S, Yoshinaka Y.** 2008. Pycnogenol, a procyanidin-rich extract from French maritime pine, inhibits intracellular replication of HIV-1 as well as its binding to host cells. Jpn. J. Infect. Dis. 61:279–285.
31. **Moolten FL.** 1986. Tumor chemosensitivity conferred by inserted herpes thymidine kinase genes: paradigm for a prospective cancer control strategy. Cancer Res. 46:5276–5281.
32. **Smith SM, Markham RB, Jeang KT.** 1996. Conditional reduction of human immunodeficiency virus type 1 replication by a gain-of-herpes simplex virus 1 thymidine kinase function. Proc. Natl. Acad. Sci. U. S. A. 93:7955–7960.
33. **Khan MA, Aberham C, Kao S, Akari H, Gorelick R, Bour S, Strebel K.** 2001. Human immunodeficiency virus type 1 Vif protein is packaged into the nucleoprotein complex through an interaction with viral genomic RNA. J. Virol. 75:7252–7265.
34. **Khan MA, Kao S, Miyagi E, Takeuchi H, Goila-Gaur R, Opi S, Gipson CL, Parslow TG, Ly H, Strebel K.** 2005. Viral RNA is required for the association of APOBEC3G with human immunodeficiency virus type 1 nucleoprotein complexes. J. Virol. 79:5870–5874.
35. **Takeuchi H, Buckler-White A, Goila-Gaur R, Miyagi E, Khan MA, Opi S, Kao S, Sokolskaja E, Pertel T, Luban J, Strebel K.** 2007. Vif counteracts a cyclophilin A-imposed inhibition of simian immunodeficiency viruses in human cells. J. Virol. 81:8080–8090.
36. **Takeuchi H, Kao S, Miyagi E, Khan MA, Buckler-White A, Plishka R, Strebel K.** 2005. Production of infectious SIVagm from human cells requires functional inactivation but not viral exclusion of human APOBEC3G. J. Biol. Chem. 280:375–382.
37. **Dettwiler S, Aringhieri C, Cardinale S, Keller W, Barabino SM.** 2004. Distinct sequence motifs within the 68-kDa subunit of cleavage factor Im mediate RNA binding, protein-protein interactions, and subcellular localization. J. Biol. Chem. 279:35788–35797.
38. **Stremlau M, Owens CM, Perron MJ, Kiessling M, Autissier P, Sodroski J.** 2004. The cytoplasmic body component TRIM5alpha restricts HIV-1 infection in Old World monkeys. Nature 427:848–853.

Teeranaipong P et al. *Journal of the International AIDS Society* 2013, **16**:18723
http://www.jiasociety.org/index.php/jias/article/view/18723 | http://dx.doi.org/10.7448/IAS.16.1.18723

JIAS Journal of the International AIDS Society

Research article

Development of a rapid cell-fusion-based phenotypic HIV-1 tropism assay

Phairote Teeranaipong*[1], Noriaki Hosoya*[2], Ai Kawana-Tachikawa[1], Takeshi Fujii[3], Tomohiko Koibuchi[3], Hitomi Nakamura[2,3], Michiko Koga[1,3], Naoyuki Kondo[4,5], George F Gao[6], Hiroo Hoshino[7], Zene Matsuda[4,5] and Aikichi Iwamoto[§,1,2,3,4]

[§]**Corresponding author:** Aikichi Iwamoto, Division of Infectious Diseases, Advanced Clinical Research Center, Institute of Medical Science, University of Tokyo, 4-6-1 Shirokanedai, Minato-Ku, Tokyo 108-8639, Japan. Tel: +81-3-6409-2202. Fax: +81-3-6409-2008. (aikichi@ra3.so-net.ne.jp, aikichi@ims.u-tokyo.ac.jp)
*These authors contributed equally to this work

Abstract

Introduction: A dual split reporter protein system (DSP), recombining *Renilla* luciferase (RL) and green fluorescent protein (GFP) split into two different constructs (DSP_{1-7} and DSP_{8-11}), was adapted to create a novel rapid phenotypic tropism assay (PTA) for HIV-1 infection (DSP-Pheno).

Methods: DSP_{1-7} was stably expressed in the glioma-derived NP-2 cell lines, which expressed CD4/CXCR4 (N4X4) or CD4/CCR5 (N4R5), respectively. An expression vector with DSP_{8-11} (pRE11) was constructed. The HIV-1 envelope genes were subcloned in pRE11 (pRE11-env) and transfected into 293FT cells. Transfected 293FT cells were incubated with the indicator cell lines independently. In developing the assay, we selected the DSP_{1-7}-positive clones that showed the highest GFP activity after complementation with DSP_{8-11}. These cell lines, designated N4R5-DSP_{1-7}, N4X4-DSP_{1-7} were used for subsequent assays.

Results: The env gene from the reference strains (BaL for R5 virus, NL4-3 for X4 virus, SF2 for dual tropic virus) subcloned in pRE11 and tested, was concordant with the expected co-receptor usage. Assay results were available in two ways (RL or GFP). The assay sensitivity by RL activity was comparable with those of the published phenotypic assays using pseudovirus. The shortest turnaround time was 5 days after obtaining the patient's plasma. All clinical samples gave positive RL signals on R5 indicator cells in the fusion assay. Median RLU value of the low CD4 group was significantly higher on X4 indicator cells and suggested the presence of more dual or X4 tropic viruses in this group of patients. Comparison of representative samples with Geno2Pheno [co-receptor] assay was concordant.

Conclusions: A new cell-fusion-based, high-throughput PTA for HIV-1, which would be suitable for in-house studies, was developed. Equipped with two-way reporter system, RL and GFP, DSP-Pheno is a sensitive test with short turnaround time. Although maintenance of cell lines and laboratory equipment is necessary, it provides a safe assay system without infectious viruses. With further validation against other conventional analyses, DSP-Pheno may prove to be a useful laboratory tool. The assay may be useful especially for the research on non-B subtype HIV-1 whose co-receptor usage has not been studied much.

Keywords: HIV-1; co-receptor; tropism; co-receptor usage; fusion; chemokine receptor.

Received 5 May 2013; **Revised** 10 August 2013; **Accepted** 19 August 2013; **Published** 18 September 2013

Introduction

A new class of drugs to combat HIV-1 infection emerged in 2007 with the marketing approval of maraviroc, a small molecule that binds specifically to the CCR5 co-receptor to block viral attachment and entry [1]. While entry inhibitors are a welcome addition to the antiretroviral arsenal, one problem with this new class of drugs is that treatment is effective only against viruses with the specified co-receptor usage. HIV-1 tropism is defined by the chemokine co-receptors used for viral attachment: R5-tropic viruses use CD4/CCR5, X4-tropic viruses use CD4/CXCR4 and R5X4- or dual-tropic viruses use both CD4/CCR5 and CD4/CXCR4 [2–4]. In clinical treatment with maraviroc, the presence of X4- or dual-tropic viruses is associated with treatment failure [5,6], and a tropism assay is mandatory before treatment initiation.

HIV-1 tropism may be examined genotypically or phenotypically. Genotypic tropism assay (GTA) is based on DNA amplification and sequencing of the third variable (V3) region of the envelope glycoprotein gp120, shown by genetic mapping to be the major determinant of HIV-1 tropism [7–10]. GTA has advantages of platform portability, low cost and rapid turnaround time [11]; however, the interpretation of the sequences is complicated because of the high variability [12]. The assay used in association with maraviroc treatment is the phenotypic tropism assay (PTA) Trofile™ (Monogram Biosciences Inc., CA, USA), a CD4 cell culture assay using replication-defective pseudoviruses [13]. Although Trofile™ is

considered the gold standard, a simpler and effective PTA would be useful.

Here, we describe a novel, cell-fusion-based PTA that uses a dual split reporter protein system (DSP) [14,15] to measure HIV-1 tropism by both Renilla luciferase (RL) activity and green fluorescent protein (GFP) activity. We validated the DSP-Pheno assay using HIV-1 reference strains and applied the assay to test clinical samples from patients with HIV-1 infection.

Methods

Approval of the study and recombinant DNA experiments

Plasma samples from HIV-1-positive patients attending the hospital affiliated with the Institute of Medical Science, the University of Tokyo (IMSUT) were collected and kept frozen until use. Patients provided written informed consent, and the study was approved by the Institutional Review Board of the University of Tokyo (approval number 20-31). Recombinant DNA experiments used in this work were approved by the Institutional Review Board (approval number 08-30), and by the review board in the Ministry of Education, Culture, Sports, Science and Technology (MEXT; approval number 23-1927).

Cell lines

Cell lines N4, N4X4 and N4R5 are derived from the human glioma NP-2 cell line and stably express CD4, CXCR4 and CCR5, respectively [16,17]. NP-2-derived cell lines were grown in M10+ medium (modified Eagle's medium (MEM; Sigma, St. Louis, MO, USA) supplemented with 10% heat-inactivated foetal bovine serum (FBS), 100 units/ml of penicillin and 0.1 mg/ml of streptomycin). 293FT cells (Invitrogen, Carlsbad, CA, USA) were grown in D10+ medium (Dulbecco's modified Eagle's medium (DMEM, Sigma) supplemented with 10% FBS, 100 units/ml of penicillin and 0.1 mg/ml of streptomycin). All cell cultures were maintained at 37°C in a humidified 5% CO_2 incubator.

Reference viral envelopes

The plasmids encoding reference HIV-1 envelopes with well-characterized co-receptor usage were obtained from NIH AIDS Research & Reference Reagent Program (NIH ARRRP: Germantown, MD, USA). NL4-3 and LAI represented X-4 tropic viruses; BaL represented R5-tropic viruses; and SF2 represented dual (R5X4)-tropic viruses. The co-receptor usage of these laboratory strains has been published [13,18–22].

Construction of DSP expression plasmids

The DSP system utilizes a pair of chimeric reporter proteins, DSP_{1-7} and DSP_{8-11}, each of which is a fusion of split green fluorescent protein (spGFP) and split Renilla luciferase (spRL) [15]. DSP_{1-7} fuses the N-terminal region of RL (amino acids 1–229) to the N-terminal region of GFP (amino acids 1–157), with a linker sequence separating the two regions. DSP_{8-11} has the complementary structure, with the C-terminal region of GFP (amino acids 158–231), fused to the C-terminal region of RL (amino acids 230–311), also separated by a linker sequence. When both reporter proteins are present in the same cell, they each recover full activity.

To generate pLenti-DSP_{1-7} plasmid, we first amplified an attB-flanked DSP_{1-7} fragment (1251 bp) using pDSP $_{1-7}$ as a template and attB-flanked primers [attB1-DSP1-1F (56-mer, 5′-GGGGACAAGTTTGTACAAAAAAGCAGGCTGGGCTAGCCACCA TGGCTTCCAAGGTG -3′) and attB2-DSP1-1R (51-mer, 5′-GG GGACCACTTTGTACAAGAAAGCTGGGTGCTCTAGATCACTTGT CGGCGG-3′)]. Sequential amplicons were transferred to pDONR-221 and pLenti6.3/V5-DEST (Invitrogen) using the ViraPower™ HiPerform™ Lentiviral Gateway® Expression System (Invitrogen) according to the manufacturer's protocol. Constructs were verified by sequencing.

An expression vector, pRE11 (Figure 1), was constructed for the co-expression of DSP_{8-11} and HIV-1 *env* by multiple rounds of PCR and subcloning. Source plasmids were pIRES2-AcGFP1 (Clontech), pmOrange (Clontech), $pDSP_{8-11}$ [15] and pmirGLO (Promega). pRE11 incorporated multiple cloning sites under the PGK promoter for the insertion of HIV-1 *env* (Shown as 5′-XbaI-XhoI-3′ in Figure 1b). Necessary restriction enzyme cleavage sites used for construction, including multiple cloning sites (XbaI-MluI-SwaI-AgeI-XhoI), were created using synthetic oligonucleotides and PCR. A CMV promoter drives $pDSP_{8-11}$ directly. The same CMV promoter expresses mOrange with a nuclear localization signal that serves as a marker for successful transfection via internal ribosomal entry site (IRES). All PCR fragments were confirmed by sequencing.

NP-2-derived fusion indicator cell lines

We used the ViraPower Packaging Mix with Lipofectamine 2000 (Invitrogen) to transfect 293FT cells with pLenti-DSP_{1-7} and create pseudoviruses containing the DSP_{1-7} expression cassette (Lenti-DSP_{1-7}). We next infected cell lines NP-2/CD4 (N4), CD4/CXCR4 (N4X4) and CD4/CCR5 (N4R5) with pseudoviruses containing LentiDSP_{1-7} for 2 hours. Cells were distributed in 96-well tissue culture plates at a density of 75 cells/plate (0.8 cell/well) and grown in the presence of 4 μg/ml blasticidin. Approximately 50 candidate clones from each cell line were randomly selected and tested for FITC intensity using FACS Calibur (BD Biosciences, Franklin Lakes, NJ, USA) 48 hours after transfection of $pDSP_{8-11}$. FACS data were analyzed by Flow Jo version 8.7.1 (Tree Star Inc., OR, USA). Clones with the highest median FITC intensity were expanded in M10+ supplemented with 4 μg/ml of blasticidin (M10 + 4) for further assays.

Generation of pRE11-env strains

Full-length HIV-1 *env* was prepared by PCR amplification from clinical plasma samples as described [23]. Viral RNA was extracted from 140 μl of patient's plasma by QIAamp Viral RNA Mini kit according to the manufacturer's recommendation (QIAGEN, Hilden, Germany). One-step RT-PCR using SuperScript III and High Fidelity Platinum® Taq DNA polymerase (Invitrogen) was carried out in five separate 15-μl reactions to minimize the bias created by PCR. The reaction mixture contained 2 μl of RNA template, 7.5 μl of 2 × reaction buffer, 0.3 μl of 5 mM $MgSO_4$, 0.3 μl of each 10 μM of forward primer (Env-1F, 25-mer, 5′-TAGAGCCCTG GAAGCATCCAGGAAG-3′) and reverse primer (Env-3Rmix, equimolar mixture of 30-mer, 5′ -TGCTGTATTGCTACTTGTGATTGCTCCATA-3′ and 30-mer, 5′ -TGCTGTATTGCTA CTTGTGATTGCTCCATG-3′), 0.6 μl of

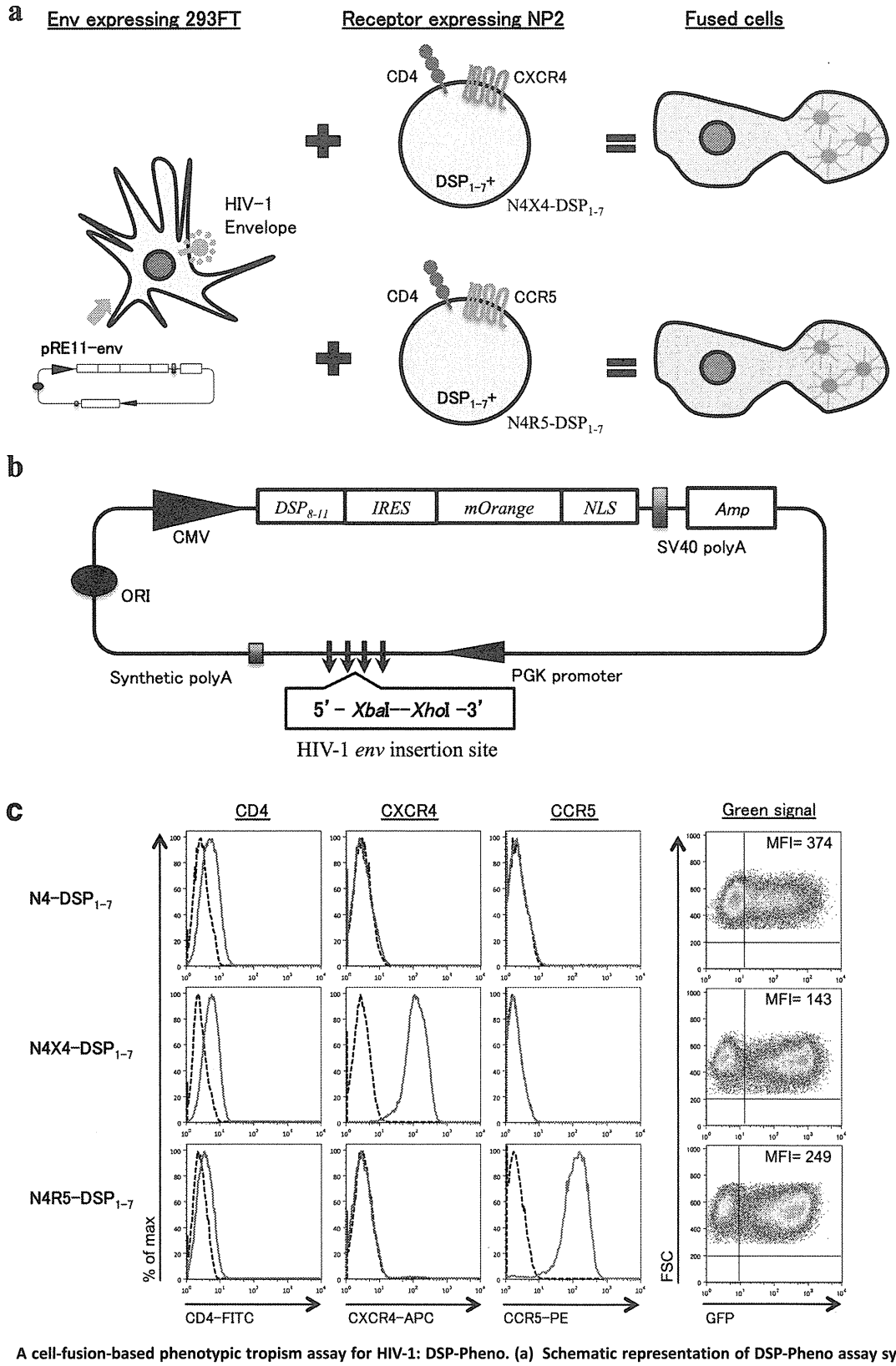

Figure 1. A cell-fusion-based phenotypic tropism assay for HIV-1: DSP-Pheno. (a) Schematic representation of DSP-Pheno assay system. (b) Schematic representation of pRE11, an expression vector for HIV-1 env and DSP_{8-11}. pRE11 encodes also mOrange with a nuclear localization signal as an indicator of transfection. (c) NP-2-derived clones stably expressing DSP_{1-7} (N4-DSP_{1-7}, N4X4-DSP_{1-7} and N4R5-DSP_{1-7}) were selected by the high GFP expression after direct transfection of $pDSP_{8-11}$. The expression of CD4/co-receptors was reconfirmed by appropriate monoclonal antibodies and FACS analysis.

SuperScript III and High Fidelity Platinum® Taq DNA polymerase, 0.25 μl of RNAse OUT and 3.75 μl of nuclease-free water with the final volume of 15 μl/reaction. The one-step RT-PCR condition was 55°C for 30 minutes, 94°C for 2 minutes followed by 30 cycles of 94°C for 20 seconds, 55°C for 30 seconds, 68°C for 4 minutes, then extension at 68°C for 5 minutes. The fragment by the first-round amplification extended from NL4-3 reference position of 5853–8936. Products from five independent reactions were combined. Four microliters of the mixed first-round PCR products were used as the template for each of five independent second-round PCR reactions employing EnvB-2F-Xba (41-mer, 5′-TAGCTCTAGAACGCGTCTTAGGCATCTCCTATGGCAG GAAG-3′) and EnvB-4R-Xho (41-mer, 5′ -TAGCCTCGAGACCGGT TACTTT TTGACCACTTGCCACCCAT-3′) as the forward and reverse primers, respectively. The second PCR was carried out according to the standard 50-μl PCR protocol of the Platinum® PCR SuperMix High Fidelity as described above. The fragments amplified by the second PCR extended from NL4-3 reference position of 5957–8817. After digestion with Xba I and Xho I, about 3-kb PCR products were purified by 1.2% agarose gel and QIAquick gel extraction kit (Qiagen). The purified products were inserted into pRE11 at XbaI and XhoI sites, resulting in HIV-1*env* expression plasmid (pRE11-envbulk) from each patient. pRE11-envbulk, representing a quasispecies of *env* population from each patient, was prepared by transfecting into *E. coli* JM109. For bulk analysis, transfected JM109 was expanded to 25 ml, followed by QIAGEN Plasmid Midi Kit (Qiagen) for DNA extraction.

Cell-fusion assay

On the day before transfection, 500 μl aliquots of 293FT cells in DMEM supplemented with 10% FBS (D10) were seeded in 24-well tissue culture plates at a density of 2.8×10^5 cells/well and incubated overnight to 70–80% confluency. The cells were then transfected with pRE11-envstrain or pRE11-envbulk according to the manufacturer's protocol (Roche). On the same day, 100 μl aliquots of N4-DSP_{1-7}, N4X4-DSP_{1-7} and N4R5-DSP_{1-7} cells in MEM supplemented with 10% FBS (M10) were seeded in a 96-well tissue culture, optical bottom plate (NUNC, Thermo Fisher Scientific Inc., NY, USA) at a density of 1×10^4 cells/well and incubated at 37°C. Forty-eight hours after transfection, the medium of transfected 293FT cells was removed by aspiration and replaced with 1 ml of PBS (Sigma) at RT. Transfected 293FT cells were resuspended by gentle pipetting.

To start the cell-fusion assay, 150 μl/well of transfected cells were overlaid onto N4-DSP_{1-7}, N4X4-DSP_{1-7} and N4R5-DSP_{1-7} cells. The cells were incubated for fusion at 37°C in a humidified 5% CO_2 incubator for 6 hours, and then analyzed by automatic image capture using an In Cell Analyzer 1000 (GE Healthcare). Four fields/well of image were captured through red, green and bright field channels, and fused cells were identified by the presence of two or more red nuclei surrounded by a green area (cytoplasm). Immediately after image capturing, EnduRen™ Live Cell Substrate (Promega) was added to each well, and luciferase activity was measured three times using a Glomax 96 microplate luminometer (Promega), according to the manufacturer's instructions. The mean luciferase activity, recorded as relative light unit (RLU), was the average of three measurements per well. The experiments were conducted in triplicates and repeated independently at least three times.

To test the co-receptor specificity, 2 μM/well of the appropriate inhibitor was added to the cells 90 minutes prior to the cell-fusion assay (CXCR4 inhibitor AMD3100 (Sigma) to N4X4-DSP_{1-7} cells and CCR5 inhibitor maraviroc (Sigma) to N4R5-DSP_{1-7} cells).

Genotyping

pRE11-envbulk were sequenced in both the 5′ and 3′ directions using population-based sequencing on the ABI 3130xl genetic analyzer (Applied Biosystems, Foster City, CA, USA) using BigDye Terminator V3.1 (Applied Biosystems) with forward primer E110 (5′ -CTGTTAAATGGCAGTCTAGCAGAA-3′), and reverse primer Er115 (5′ -AGAAAAATTCCCCTCCACAATT AA-3′). The V3 nucleotide sequences were submitted to the Geno2Pheno (co-receptor) algorithm (http://coreceptor.bioinf.mpi-inf.mpg.de) setting the false positive rate (FPR) at 10%.

Results

Construction of DSP_{1-7} and DSP_{8-11} expression vectors

We inserted DSP_{1-7} or DSP_{8-11} sequences into blasticidin-resistant lentivirus vectors and then infected NP-2/CD4 (N4), NP-2/CD4/CXCR4 (N4X4) and NP-2/CD4/CCR5 (N4R5) cells with the recovered pseudoviruses, selecting for blasticidin-resistant clones. We screened 49, 51 and 43 lentivirus-infected and blasticidin-resistant clones from N4, N4X4 and N4X5, respectively, for high levels of DSP_{1-7} or DSP $_{8-11}$ expression following super-transfection with the complementary plasmid (pDSP_{8-11} or pDSP_{1-7}, respectively). From each of the cell lines, we selected the blasticidin-resistant and DSP_{1-7}-positive clone that showed the highest GFP activity after complementation with DSP_{8-11}. These cell lines, designated N4-DSP_{1-7}, N4X4-DSP_{1-7} and N4R5-DSP_{1-7}, were re-evaluated for their expression of CD4, CXCR4 and CCR5 on the cell surface (Figure 1c).

Using this approach, we obtained N4- and N4R5-cells expressing high levels of DSP_{8-11}, but were unable to obtain a stable N4X4 cell line expressing DSP_{8-11} (data not shown). To circumvent this problem, we decided to generate 293FT cells transiently expressing both DSP_{8-11} and the HIV-1 *env* protein and develop a cell-fusion assay system using those cells together with the NP-2-derived cells stably expressing DSP_{1-7} (Figure 1a). Thus, we constructed the expression vector pRE11, containing the DSP_{8-11} expression cassette and cloning sites for insertion of HIV-1 *env* sequences under the control of the PGK promoter (Figure 1b).

Validation of the cell-fusion assay using the *env* gene from laboratory HIV-1 strains

We validated the DSP assay system (DSP-pheno) using pRE11 constructs engineered to contain *env* sequences from reference strains with known co-receptor usage. The *env* reference constructs, which also contained the DSP_{8-11} expression cassette, were the following: pRE11-HXB2, pRE11-LAI, and pRE11-NL4-3 (X4 strains); pRE11-BaL (R5 strain); and pRE11-SF2 (dual strain). The cell-fusion assays were performed with N4X4-DSP_{1-7} or N4R5-DSP_{1-7} cells in

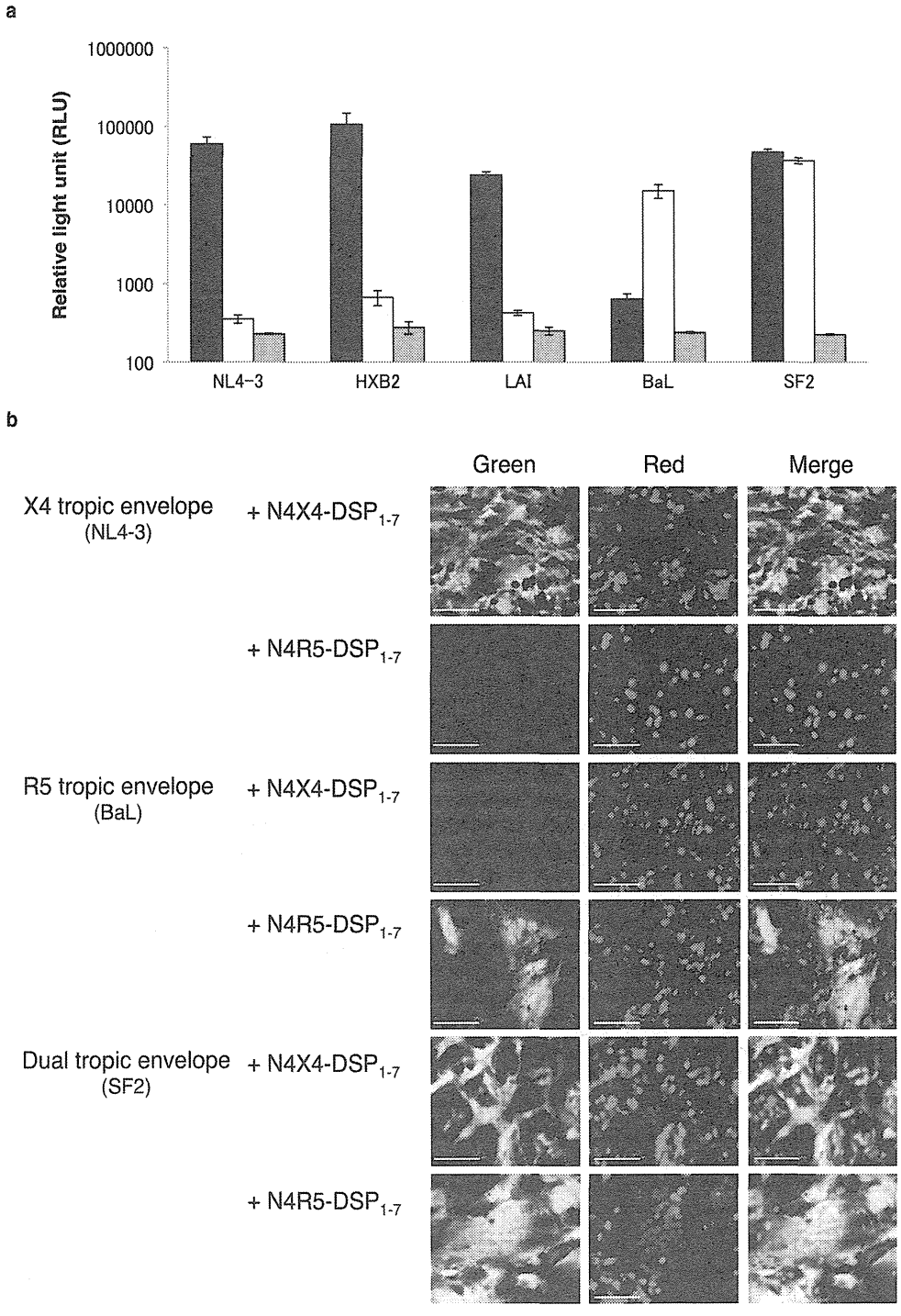

Figure 2. Validation of the cell-fusion assay using env genes from HIV-1 reference strains. (a) RL activities after cell fusion were measured using NL4-3, HXB2 and LAI as X4 reference strains while BaL or SF2 as R5 or R5X4 strains, respectively. Black columns: RL activities on N4X4-DSP_{1-7}. White columns: activities on N4R5-DSP_{1-7}. Grey columns: activities on N4-DSP_{1-7}. Small bars at the top of each column indicate the mean RLU ± SD from three independent experiments. (b) Successful cell fusion is indicated by the green fluorescence in the cytoplasm. Red spots were mOrange activity in the nuclei showing successful transfection. Merged images showed multinuclear cells with multiple yellow/orange nuclei surrounded by green cytoplasm.

combination with 293FT cells transiently expressing one of the pRE11-env constructs. In all the assays, both RL and GFP activities were restored only when cells expressing the appropriate *env* and co-receptor combinations were co-cultured (Figure 2a and b). Co-culture of N4X4-DSP_{1-7} or N4R5-DSP_{1-7} in combination with the 293FT cells transiently expressing the pRE11-env constructs of discordant tropism served as a negative control for expression of RL activities